TECHNICAL REPORT STANDARD PAGE

1. Title and Subtitle

Estimating HCM Default Parameters for Louisiana

2. Author(s)

M. Ashifur Rahman, Ph.D.; Milhan Moomen, Ph.D.;
Siam Junaed, E.I.

3. Performing Organization Name and Address

Louisiana Transportation Research Center

4101 Gourrier Avenue

Baton Rouge, LA 70808

4. Sponsoring Agency Name and Address

Louisiana Department of Transportation and Development

P.O. Box 94245

Baton Rouge, LA 70804-9245

5. Report No.

FHWA/LA.25/715

6. Report Date

July 2025

7. Performing Organization Code

LTRC Project Number: 23-3SS

SIO Number: DOTLT1000459

8. Type of Report and Period Covered

Final Report

01/2023 – 04/2025

9. No. of Pages

101

13. Abstract

Although the Highway Capacity Manual (HCM) provides default values for its methodologies, it also
states that these values represent typical national values and that conditions within a state, region, or
community may differ. When default values are applied frequently in analyses, the use of local
default values can reduce the uncertainty in the analysis results. This study addresses the need for
accurate intersection capacity analysis in Louisiana, where reliance on default Highway Capacity
Manual (HCM) values can lead to inefficiencies due to regional variations in traffic conditions. The
research focused on estimating key traffic flow parameters: base saturation flow rate (BSFR) for
signalized intersections, and critical headway (CH) and follow-up headway (FH) for two-way stop-
controlled (TWSC) intersections. A comprehensive database for signalized and stop-controlled
intersections was developed by integrating data from multiple sources, including the extensive traffic
data collection 511 system, highway database, and DOTD representatives. The study analyzed 51
signalized intersections, adjusting for factors such as lane width, heavy vehicle presence, and turning

movements. This resulted in a statewide BSFR of 1,655 pc/h/ln, lower than the HCM default. Significant regional differences were observed, with district-specific BSFRs ranging from 1,537 pc/h/ln to 1,773 pc/h/ln. For TWSC intersections, data from 26 four-leg intersections were used to estimate CH (7.1 to 10.1 sec.) and FH (5.9 to 6.5 sec.), which were both substantially higher than HCM defaults, reflecting conditions at low-volume minor roads. The study highlights the limitations of applying national default values and emphasizes the importance of using locally estimated parameters for more effective traffic management. The findings support the adoption of district-specific BSFRs for signal timing and capacity analysis, as well as the application of the estimated CH and FH values for TWSC intersection design, with appropriate HCM adjustments.

Project Review Committee

Each research project will have an advisory committee appointed by the LTRC Director. The Project Review Committee is responsible for assisting the LTRC Administrator or Manager in the development of acceptable research problem statements, requests for proposals, review of research proposals, oversight of approved research projects, and implementation of findings.

LTRC appreciates the dedication of the following Project Review Committee members in guiding this research study to fruition.

LTRC Administrator/Manager
Julius Codjoe, Ph.D., P.E.
Special Studies Research Administrator

Members
Mathilda Rilovich
John Broemmelsiek
Natalie Sistrunk
Cristine Gowland
Ben Boudreaux
Angela Murrell

Directorate Implementation Sponsor
Chad Winchester, P.E.
DOTD Chief Engineer

Estimating HCM Default Parameters for Louisiana

By

M. Ashifur Rahman, Ph.D.
Milhan Moomen, Ph.D.
Siam Junaed, E.I.

Louisiana Transportation Research Center
4101 Gourrier Avenue
Baton Rouge, LA 70808

LTRC Project No. 23-3SS
SIO No. DOTLT1000459

conducted for

Louisiana Department of Transportation and Development
Louisiana Transportation Research Center

July 2025

Abstract

Although the Highway Capacity Manual (HCM) provides default values for its methodologies, it also states that these values represent typical national values and that conditions within a state, region, or community may differ. When default values are applied frequently in analyses, the use of local default values can reduce the uncertainty in the analysis results. This study addresses the need for accurate intersection capacity analysis in Louisiana, where reliance on default Highway Capacity Manual (HCM) values can lead to inefficiencies due to regional variations in traffic conditions. The research focused on estimating key traffic flow parameters: base saturation flow rate (BSFR) for signalized intersections, and critical headway (CH) and follow-up headway (FH) for two-way stop-controlled (TWSC) intersections. A comprehensive database for signalized and stop-controlled intersections was developed by integrating data from multiple sources, including the extensive traffic data collection 511 system, highway database, and DOTD representatives. The study analyzed 51 signalized intersections, adjusting for factors such as lane width, heavy vehicle presence, and turning movements. This resulted in a statewide BSFR of 1,655 pc/h/ln, lower than the HCM default. Significant regional differences were observed, with district-specific BSFRs ranging from 1,537 pc/h/ln to 1,773 pc/h/ln. For TWSC intersections, data from 26 four-leg intersections were used to estimate CH (7.1 to 10.1 sec.) and FH (5.9 to 6.5 sec.), which were both substantially higher than HCM defaults, reflecting conditions at low-volume minor roads. The study highlights the limitations of applying national default values and emphasizes the importance of using locally estimated parameters for more effective traffic management. The findings support the adoption of district-specific BSFRs for signal timing and capacity analysis, as well as the application of the estimated CH and FH values for TWSC intersection design, with appropriate HCM adjustments.

Acknowledgements

Implementation Statement

Transportation planners in Louisiana will gain critical insights into traffic flow at signalized and stop-controlled intersections, improving network-level planning and simulation accuracy. This study helps prevent inaccurate capacity and traffic flow estimates, supporting better decision-making. However, the commonly used base saturation flow rate (BSFR), along with critical headway (CH) and follow-up headway (FH), often fails to reflect localized traffic conditions due to deteriorating traffic and evolving vehicle performance, which alters driving behavior. Inaccurate parameters can lead to inefficient traffic operations, miscalculated fair share contributions, and suboptimal signal timings, resulting in defective green time splits and offsets in coordinated signals. Applying nationwide values for these parameters is unsuitable for intersections with unique driving behaviors and traffic conditions. A deeper understanding of local HCM parameters will enhance capacity estimates and inform future intersection improvements. This will enable planners to design intersections and signal timings more effectively, potentially reducing congestion.

Table of Contents

List of Tables

List of Figures

Introduction

Intersections are key components of the traffic network, enabling the movement of drivers, pedestrians, and bicyclists across routes. Intersection capacity, defined as the maximum number of vehicles passing through an intersection in a given time, influences road network efficiency. It affects traffic flow and throughput, indicating the number of vehicles traveling through an intersection within a specified period. Intersection capacity also relates to congestion and delay, reflecting the time vehicles wait before proceeding [1]. Planning, design, operation, and management decisions of a road network depend on intersection capacity [2].

Intersection capacity depends on geometric design, traffic control measures, weather conditions, and other factors. Traffic performance and level of service at an intersection are assessed through the relationship between delay or queue length and capacity [3]. Measuring the capacity of an existing intersection under real-world traffic conditions is challenging. To estimate intersection capacity, parameters must be determined based on the intersection type.

Intersection capacity parameters include saturation flow rate (SFR), critical headway (CH), and follow-up headway (FH). SFR is used for signalized intersections, while CH and FH estimate the capacity of stop-controlled intersections. Estimation of these parameters influences traffic flow analysis. Capacity estimation allows planners to design and manage intersections by predicting congestion, optimizing signal timings, and deciding on infrastructure improvements.

The Highway Capacity Manual (HCM) outlines concepts, guidelines, and procedures for computing the capacity and level of service of highway facilities, including highways, transit, bicycle, and pedestrian facilities [4]. It provides methodologies for estimating and measuring the capacity of signalized and stop-controlled intersections, along with default values for intersection capacity parameters. These default values are used instead of field data to evaluate intersection capacity. Research indicates that default values may not represent local conditions and highlights the need for region-specific data to improve capacity computations [5] [6]. The HCM notes that intersection capacity parameters at locations can differ from national averages due to regional or site-specific characteristics.

SFR is a parameter for estimating the capacity and performance of signalized intersections. It aids in designing signal timings to manage traffic flow at junctions [7]. SFR is influenced by factors such as the number and width of lanes, lane usage, roadway grades, and constraints

like conflicting vehicle or pedestrian traffic, on-street parking, and bus operations. Saturation flow rates vary by movement, time, and location. The SFR at an intersection can differ from the ideal SFR values in the HCM [7]. Research shows that the base SFR in regions often deviates from the HCM's recommended value of 1,900 passenger cars per hour per lane (pc/hr/ln) [6] [8] [9] [10].

CH and FH are important gap acceptance parameters at stop-controlled intersections, influencing capacity and safety [11]. CH is the minimum time interval in the major traffic stream needed for one minor street vehicle to enter, while FH is the time gap between the departure of one minor street vehicle and the next, using the same gap in major street traffic, assuming continuous queuing on the minor street. These parameters depend on driver behavior and traffic conditions, affecting traffic performance and efficiency. HCM suggests CH values from 4.1 to 7.3 sec. and FH values from 2.2 to 4 sec. Studies show differences between observed CH and FH values and HCM-recommended values, indicating the need for region-specific data to improve accuracy [12].

Louisiana's traffic conditions are influenced by its geographical, cultural, and economic factors, with roadway infrastructure serving commuters and freight traffic across diverse regions, where varying roadside development impacts traffic dynamics. These factors warrant the development of localized intersection capacity parameters to enhance traffic analysis accuracy and reflect Louisiana's unique conditions. Estimated intersection capacity parameters with locally observed data will facilitate network-level planning and optimize transportation system performance. Short-term transportation improvement programs, spanning a 4-year horizon, and long-range transportation plans at both the statewide and metropolitan levels, covering a 20-year horizon, evaluate roadway system performance to identify infrastructure improvements based on projected demand, while targeted corridor assessments by state and local agencies address intersection safety and operational concerns to enhance system performance in priority areas [13]. Through an ongoing effort to implement Transportation Systems Management and Operations (TSMO) in Louisiana, agencies are analyzing regional transportation as an interconnected network, improving traveler and system performance through better management of the multimodal system, where updated intersection capacity estimates can further support these initiatives.

Literature Review

To advance the effort to effectively estimate intersection capacity parameters, a comprehensive review was conducted to gain insights from past studies on the estimation of intersection capacity parameters across the United States and other countries. This review focused on exploring the methodologies used to estimate these parameters and factors identified influencing them. The review involved a thorough examination of peer-reviewed journals, as well as state and federal reports documenting relevant research, with special emphasis on studies based on empirical data collected from field installations rather than theoretical approaches. The remaining sections of the literature review are divided according to the intersection types: signalized intersections (SFR) and stop-controlled intersections (CH and FH).

Signalized Intersections

Saturation flow rate (SFR) is a fundamental parameter in determining the capacity of signalized intersections. As defined by the Highway Capacity Manual (HCM), SFR is the number of vehicles per hour per lane that could pass through a signalized intersection if a green signal was displayed for the full hour, the flow of vehicles never stopped, and there were no large headways. The HCM provides guidelines for estimating SFR and recommends a base value of 1,900 passenger cars per hour per lane (pc/h/ln), which is commonly applied in practice. However, this base value may not fully reflect localized traffic conditions, as the HCM acknowledges that input parameters can vary based on regional characteristics. To address this, numerous studies have estimated region-specific SFRs using both HCM-recommended methods and alternative approaches developed by researchers. Several of these studies have highlighted the importance of accurate SFR estimation for effective transportation planning and have identified additional factors, beyond those considered in the HCM, that significantly influence SFR. The following section provides a comprehensive review of relevant findings from these studies.

Methodologies Adopted to Estimate SFR

Several methods are available for estimating SFR, each offering distinct advantages depending on data availability, traffic conditions, and technological resources. A commonly used method is field measurement, which involves collecting data directly from intersections

through on-site observations and manual counts of vehicle movements during the green signal phase. Another widely applied approach is regression analysis, wherein statistical models are used to estimate SFR based on various influencing factors such as lane width, traffic composition, and area type. With advancements in technology, real-time data collection methods have also emerged, enabling dynamic and continuous estimation of SFR under varying traffic conditions. Each of these methods presents specific strengths and limitations, and their applicability depends on the context and objectives of the SFR estimation. The following sections provide a detailed description of these methods.

HCM Methodologies. The Highway Capacity Manual (HCM) outlines two primary methods for estimating SFR: the adjustment method and the saturation headway/field measurement method. The adjustment method begins with a base saturation flow rate of 1,900 pc/h/ln, which assumes ideal conditions, including a 12-ft. lane width, absence of heavy vehicles, flat grade, no on-street parking, no bus stops, uniform lane utilization, and no turning vehicles [11]. This base value is then modified using adjustment factors to account for site-specific conditions such as lane width, approach grade, heavy vehicle percentage, and other geometric and operational attributes; see Equation 1. This method is especially useful for generating quick SFR estimates in scenarios where detailed field data is unavailable.

$$s = s_0\, f_w\, f_{HVg}\, f_p\, f_{bb}\, f_a\, f_{LU}\, f_{LT}\, f_{RT}\, f_{Lpb}\, f_{Rpb}\, f_{wz}\, f_{ms}\, f_{sp} \tag{1}$$

where,
s = base saturation flow rate (pc/h/ln);
f_w = adjustment factor for lane width;
f_{HVg} = adjustment factor for heavy vehicles in traffic stream and approach grade;
f_p = adjustment factor for the existence of a parking lane and parking activity adjacent to the lane group;
f_{bb} = adjustment factor for blocking effect of local buses that stop within the intersection area;
f_a = adjustment factor for area type;
f_{LU} = adjustment factor for lane utilization;
f_{LT} = adjustment factor for left-turn vehicle presence in a lane group;
f_{RT} = adjustment factor for right-turn vehicle presence in a lane group;
f_{Lpb} = pedestrian-bicycle adjustment factor for left-turn groups;
f_{Rpb} = pedestrian-bicycle adjustment factor for right-turn groups;
f_{wz} = adjustment factor for work zone presence at the intersection;
f_{ms} = adjustment factor for downstream lane blockage; and
f_{sp} = adjustment factor for sustained spillback.

The field measurement method, also known as the saturation headway method, estimates the SFR by taking the reciprocal of the average saturation headway. Saturation headway is defined as the average time gap between vehicles in a queue, measured after the fourth vehicle and continuing until the last vehicle in the initial queue clears the signalized intersection [11]. This approach requires direct observation and measurement of traffic flow during the green phase at a specific intersection. Headways are typically recorded starting from the fourth vehicle to exclude the effects of start-up delay and acceleration associated with the lead vehicles, thereby providing a more stable representation of normal traffic flow conditions. The mean headway, averaged over multiple signal cycles, is then used to compute the SFR using a defined formula; see Equation 2. This method is particularly valuable when a detailed, accurate, and site-specific estimation of SFR is required.

$$S = \frac{3600}{h_s} \tag{2}$$

where,

h_s = Saturation headway.

TRRL Method. The Transport and Road Research Laboratory (TRRL) developed a method for estimating saturation flow at signalized intersections that relies on classified vehicle counts without the need to convert vehicles into Passenger Car Units (PCU) [14]. This method involves observing three saturated green intervals and recording the number of vehicles passing through the intersection during each interval. The SFR is then calculated by dividing the number of vehicles in the middle interval, which is assumed to best represent stable flow, by the duration of that interval. This approach provides a simplified and practical means of estimating saturation flow using basic observational data.

Regression Method. The regression method for estimating SFR [15] [16] [17] [18] involves analyzing the relationship between traffic flow variables, with SFR as the dependent variable and factors such as saturated green time, vehicle classifications, and lost time as independent variables. By applying regression analysis, predictive models are developed to estimate SFR based on these inputs, enabling site-specific adjustments and providing insights into how various conditions influence intersection capacity. Researchers have extensively applied regression techniques to identify and quantify the impact of different factors on SFR [19] [20] [21] [22]. Specifically, multiple linear regression is commonly employed to develop

predictive models that incorporate a wide range of influencing parameters, allowing for adaptation to specific traffic, geometric, and operational characteristics [23] [24].

Other Methods. In recent years, researchers have utilized real-time data and advanced analytical techniques, such as neural networks, to estimate SFR. For example, Qi and Hu [25] developed a real-time SFR estimation model using loop detector data combined with a Markov Chain framework to capture traffic headway states. Their model utilizes a Hidden Markov Model (HMM) to identify stable headways within each signal cycle, effectively transforming SFR estimation into a state identification problem. Similarly, Wang et al. [26] proposed an automated video-based method for estimating SFR, modeling vehicle headways as a time series and applying ordinary least squares (OLS) regression to estimate key parameters. Their approach includes an iterative quantile-based filtering technique to remove abnormal data and improve accuracy.

Building upon these advancements, Wang et al. introduced a neural network-based model to dynamically account for variations in SFR and its influencing factors [27]. By analyzing traffic flow characteristics, the model was trained and validated, demonstrating its adaptability to fluctuating traffic conditions. In the context of developing countries, where heterogeneous and mixed traffic conditions are prevalent, traditional methods such as those prescribed by the HCM may be insufficient. To address this issue, Mondal et al. developed an optimization-based model for estimating Passenger Car Unit (PCU) values and saturation flow under mixed traffic conditions [18]. Their regression-based prediction model, validated using field data, demonstrated high accuracy and applicability in complex traffic environments.

Factors Affecting SFR

SFR is influenced by a wide range of factors, encompassing both the geometric and operational characteristics of intersections, as well as regional traffic conditions. While the HCM provides standardized adjustment factor values, these may not adequately capture localized variations in certain contexts [10]. Moreover, several studies have identified additional factors that significantly impact SFR but are not accounted for in the HCM framework [6] [9] [28]. As such, a comprehensive understanding of these influencing factors is essential for accurate and context-specific SFR estimation. This section reviews the key factors affecting SFR as identified in prior research.

Geometric Factors

Effect of the number of lanes. The influence of the number of lanes on SFR has been extensively examined, with consistent findings reported across multiple studies [9] [28] [29]. In general, SFR increases with the number of lanes on an approach. For example, McMahon et al. [28] found that the SFR for through movements on three-lane approaches was approximately 1,910 pc/h/ln, compared to 1,790 pc/h/ln for two-lane approaches and 1,670 pc/h/ln for single-lane approaches. Figure 1 illustrates the adjustment factors based on these results, derived using a base SFR of 1,800 pc/h/ln. Similarly, Bester et al. [29] reported that increasing the number of through lanes from one to two significantly improved SFR. Additionally, Bonneson et al. observed that individual lanes within a multi-lane approach may exhibit varying SFRs, with curb lanes often displaying lower values due to external friction caused by nearby driveways, pedestrians, and roadside elements [9]. Overall, the findings indicate that increasing the number of lanes generally leads to a higher average SFR across all lanes.

Figure 1. Adjustment factor for number of lanes based on McMahon data [28]
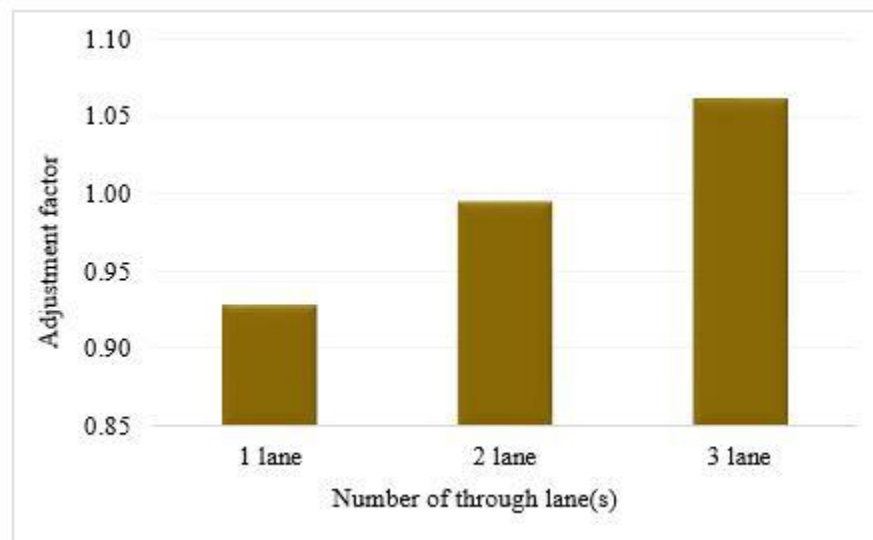
Effect of lane width. Lane width is a significant factor influencing SFR, as recognized by the HCM. The HCM provides adjustment factors to account for the negative impact of narrower lanes and the positive impact of wider lanes on SFR, as outlined in Exhibit 19-20 of the 7th edition. These findings have been supported by several researchers. Potts et al. [30] observed that narrow lanes reduce SFR by approximately 4.3% compared to standard lane

widths (3.3–3.6 m), while wider lanes (4.0 m or more) increase SFR by approximately 4.4%. Shao et al. [31] also highlighted the substantial influence of lane width, particularly on the SFR of exclusive lanes. However, Dunlap [10] noted that the HCM's adjustment factors may be inadequate in certain locations, underscoring the importance of using locally calibrated data to more accurately reflect site-specific conditions.

Effect of turning radius. The influence of turning radius on SFR has been emphasized in several studies [31] [32] [33]. Although the HCM provides adjustment factors for right- and left-turning movements, these do not explicitly account for the effect of turning radius. Bonneson noted that the HCM tends to underestimate the impact of sharp radii and overestimate the influence of flatter radii, potentially leading to inaccurate capacity estimates. In his study, Zegeer [33] proposed equivalency factors of 1.19 for right-turning movements with a turning radius less than 30 ft. and 1.10 for larger radii, compared to the HCM's recommended factor of 1.18, highlighting discrepancies in existing guidelines. Additionally, Shao et al. [31] found that turning radius has a significant effect on the capacity of exclusive turn lanes, with capacities decreasing when the radius falls below 45 m. Based on these findings, researchers recommend that turning radius be explicitly considered as a critical factor when estimating SFR, especially for turn lanes, to ensure more accurate capacity assessments.

Effect of approach grade. Previous studies have demonstrated that approach grade significantly influences SFR [29], with uphill slopes generally reducing SFR due to slower vehicle acceleration and downhill slopes increasing it as a result of higher approach speeds. The HCM addresses this effect by providing adjustment factors (see Exhibits 19-9 and 19-10 of the HCM) to account for changes in vehicle performance on grades. However, several researchers have argued that the actual impact of gradient on SFR is greater than what the HCM adjustment factors suggest [29] [34].

Effect of pedestrian crossing. Pedestrian conflicts can have a significant impact on vehicle turning movements at intersections, particularly for right-turning vehicles. Roshani et al. [35] examined the effect of pedestrian volume on the SFR of right-turn movements at signalized intersections and identified a linear relationship between pedestrian flow and SFR, with higher pedestrian volumes leading to reduced vehicle flow. This reduction occurs as vehicles are often required to yield to pedestrians in the crosswalk, disrupting the continuity of traffic flow. Similarly, Zegeer [33] found that the adjustment factor for basic right-turn movements, recommended as 0.85 by the HCM, should be further reduced in proportion to the volume of conflicting pedestrians.

Traffic Composition

Effect of right-turning vehicles. The presence of right-turning vehicles affects the SFR in both shared through and right-turn lanes as well as exclusive right-turn lanes. As the proportion of right-turning vehicles in the traffic stream increases, SFR tends to decrease due to additional lane-changing conflicts and reduced lane utilization efficiency [9]. However, Bonneson et al. [9] observed that the actual impact of right-turning vehicles on SFR is less severe than indicated by the HCM, suggesting that the HCM may overestimate their negative effects on intersection capacity.

Effect of heavy vehicles. Heavy vehicles, due to their larger size and distinct operational characteristics compared to passenger cars, have a notable impact on SFR within traffic streams. Bonneson et al. [9] found that the presence of heavy vehicles, such as trucks and buses, reduces SFR, with the extent of the reduction increasing proportionally with their percentage in the traffic flow. McMahon et al. [28] further quantified this impact, reporting that the presence of a single heavy vehicle in the queue can lead to an 8–11% decrease in SFR.

Effect of non-local drivers. Zhao et al. [36] investigated the impact of non-local drivers, defined as drivers unfamiliar with the roadway facility, on SFR at signalized intersections. Their findings revealed that intersections with a high proportion of non-local drivers experienced up to a 19% reduction in SFR. This effect is particularly relevant in recreational or tourist areas, where a substantial number of non-local drivers are present, highlighting the importance of considering driver familiarity as a factor in SFR estimation.

Environmental Conditions

Effect of side friction. Various sources of side friction, including driveways, pedestrians, roadside developments, signage, utility poles, and other roadside objects located near moving traffic, have been shown to significantly reduce SFR of rightmost (i.e., curbside) lanes. Bonneson et al. [9] observed that the curb lane within a through lane group typically exhibits a lower SFR compared to adjacent lanes. Similarly, McMahon et al. [28] reported that high levels of side friction can lead to a 3–11% reduction in SFR in the rightmost through lane relative to the leftmost lane. These findings emphasize the importance of accounting for roadside friction when estimating SFR, particularly in urban environments where such disruptions are more prevalent.

Effect of weather. A study conducted by Dunlap [10] demonstrated that weather conditions have a measurable impact on SFR. Data collected from the same intersections under both dry and rainy conditions revealed that the average SFR during dry conditions was 1,717 pc/h/ln, whereas rainy conditions resulted in a reduced SFR of 1,646 pc/h/ln, indicating a decline of approximately 70 pc/h/ln. Figure 2 illustrates the comparison of SFR during dry and wet conditions. Similarly, Sun et al. conducted a study in China and found that saturation flow decreased by 3–7% during rainy weather compared to clear conditions [37]. These findings establish a clear relationship between weather conditions and SFR, emphasizing the need to adjust ideal SFR values in regions with frequent adverse weather to improve the accuracy of capacity estimates and enhance traffic management strategies.

Figure 2. Comparison of SFR during dry and wet conditions [10]
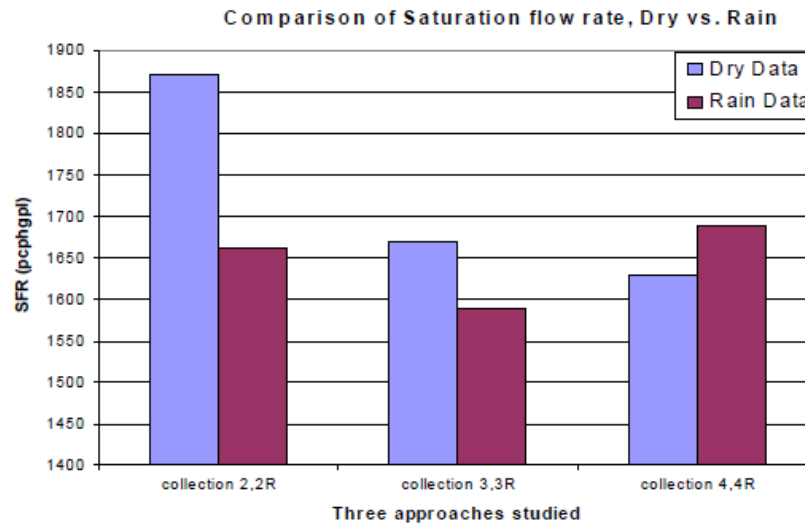
Regulatory Factors

Effect of speed limit. Studies have shown that speed limits have a significant influence on SFR, with higher speed limits generally associated with increased SFR, and lower speed limits resulting in reduced flow rates [29] [38] [39]. A study by the Texas Transportation Institute [9] reported that SFR decreases by approximately 9 pc/h/ln for every 1 mph (equivalent to 5.6 pc/h/ln per 1 km/h) reduction in speed limit. Similarly, Bester and Meyers [29] conducted a study in South Africa and found that SFR increases by 8.5 pc/h/ln per 1 km/h increase in speed limit. Despite this observed relationship, the HCM does not currently account for speed limits in its SFR estimation procedures. These findings suggest the need to

incorporate speed limit adjustments into SFR estimation methodologies to improve the accuracy of capacity assessments, particularly in areas with varying posted speed limits.

Effect of camera enforcement. A study by Al-Mistarehi et al. [32] conducted in Jordan identified camera enforcement as a unique and significant factor affecting SFR. The presence of enforcement cameras was found to influence driver behavior, making drivers more cautious and reducing the incidence of red-light violations. While this enhances safety, it also results in a lower number of vehicles clearing the intersection during the green phase, thereby leading to a reduction in SFR.

Effect of traffic pressure. Previous studies have extensively examined the impact of traffic pressure, often quantified by queue length, on SFR. Traffic pressure is typically characterized by more aggressive driver behavior, particularly during high-volume periods such as rush hours, in which drivers aim to minimize travel time by accepting shorter headways during queue discharge. Bonneson [40] found that longer queues at intersections are associated with higher SFRs, as aggressive driving behavior leads to reduced headways. In a subsequent study, Bonneson and Messer [39] developed a traffic-pressure adjustment factor to account for the influence of traffic volume on SFR. Their findings indicated that intersections with lower volumes and shorter queues generally exhibit lower SFRs, while intersections with higher volumes and longer queues experience increased SFRs due to heightened traffic pressure. This phenomenon highlights a positive relationship between traffic volume and SFR, driven by behavioral adaptations in high-demand conditions, as illustrated in Figure 3.

Figure 3. Traffic pressure adjustment factors [39]
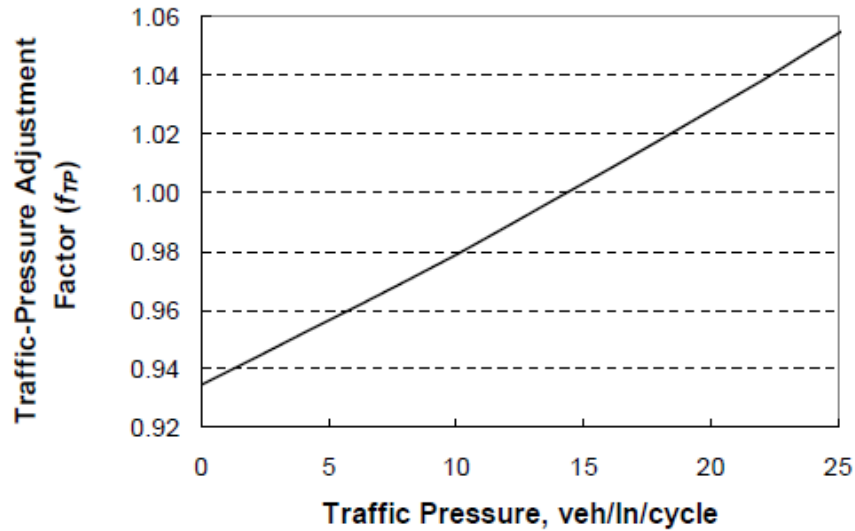
Demographic Factors

Effect of area population. Area population, defined as the number of residents in the vicinity of an intersection or roadway facility, has been identified by several researchers as a significant factor influencing SFR [6] [33] [41]. Findings suggest that SFR tends to be lower in areas with smaller populations, potentially due to differences in driving behavior, roadway familiarity, and traffic demand. Zegeer proposed adjustment factors based on population size: 1.00 for areas with populations over 100,000, 0.91 for populations between 20,000 and 100,000, and 0.83 for populations under 20,000 [33]. Similarly, Cartagena et al. reported that SFR in medium-sized towns was approximately 8% lower than in large towns and 21% lower in small towns [6]. They recommended adjustment factors of 0.92 for medium towns and 0.79 for small towns. Although the HCM does not currently consider area population in its SFR estimation procedures, these studies indicate that population size may serve as a meaningful predictor, particularly in regions with varying population densities. Incorporating this factor could improve the accuracy of SFR estimates in diverse geographic contexts.

Effect of area type. The Highway Capacity Manual (HCM) includes an adjustment factor of 0.90 to account for the reduced efficiency of intersections located in central business districts (CBDs). This factor reflects the generally lower SFRs observed in these areas due to increased pedestrian activity, constrained geometry, and higher variability in driver behavior.

However, several studies have evaluated the relationship between SFR and area type, finding that while SFRs in CBDs are indeed lower, the adjustment factors derived from empirical data often differ from the HCM's recommendation [33] [41] [42]. Table 1 provides a comparison between the adjustment factors suggested by the HCM and those identified in the literature for various area types. For instance, Le et al. [20] and Zegeer [33] found that residential areas typically exhibit higher SFRs compared to outlying commercial districts and CBDs, likely due to less congestion, fewer conflicts, and more familiar driving environments. Additionally, Le et al. [20] reported that recreational areas show significantly lower SFRs, similar to those observed in CBDs. This reduction is attributed to the high proportion of non-local drivers in recreational areas, whose unfamiliarity with the roadway system contributes to longer headways and more cautious driving behavior.

Table 1. Comparison of area type adjustment factor

Studies	Residential	CBDs	Recreational
HCM [11]	1	0.9	Not available
Le et al. [20]	1	Not available	0.92
Zegeer [33]	1.01	0.99	Not available
Agent and Crabtree [41]	1	0.97	Not available

To further summarize the key findings, two reference tables are provided below. Table 2 outlines the various factors influencing SFR, along with the corresponding methods used to estimate them, based on the studies reviewed in this section. Table 3 highlights additional variables that have been identified in the literature as having a significant impact on SFR, but that are not currently accounted for in HCM. Together, these tables provide a concise and organized reference to support the detailed discussion presented above, enhancing understanding of both established and emerging factors that influence SFR and highlighting opportunities for improved capacity estimation practices.

Table 2. Summary of factors affecting SFR

Factors	Methodology	Location	Reference
Traffic pressure, number of lanes, speed limit	Linear regression analysis Sensitivity analysis	Florida USA	[9]
Turning radius, area population, area type	-	USA	[33]
Area type	ANOVA	Florida USA	[20]
Heavy vehicle, side friction, number of lanes	Statistical analysis	South Florida USA	[28]
Lane type, lane width, grade, heavy vehicles	ANOVA	Pennsylvania USA	[10]
Size of town	Weighted linear regression	Indiana USA	[24]
Non-local driver	One way ANOVA	Florida USA	[36]
Lane width	ANOVA	USA	[30]
Lane width, approach grade, turning radius, vehicle type	Partial least-square method	China	[31]
Weather	ANOVA	China	[37]
Speed limit, number of through lane, grade	Multiple linear regression	South Africa	[29]
Camera enforcement, speed limit, turning radius	Multiple linear regression	Jordan	[32]
Speed limit, lane marking, city, location (CBD/non-CBD)	ANOVA	Kuwait	[38]
Pedestrian crossing	Regression models	Iran	[35]

Table 3. Factors affecting SFR considered in HCM and other studies

Factors	HCM	Studies
Number of lanes		[9], [28], [29]
Lane width	✓	[10], [30]
Turning radius		[31], [32], [33]
Approach grade	✓	[29], [34]
Pedestrian	✓	[35]
Right-turn movement	✓	[9]
Heavy vehicle	✓	[9], [28]
Non-local driver		[36]
Side friction	✓	[9], [28]
Weather		[10]
Speed limit		[9], [29], [38], [39]
Camera enforcement		[32]
Traffic pressure		[9], [39], [40]
Area population		[6], [33], [41]
Area type	✓	[20], [33]

SFR Estimation and Regional Discrepancies

SFR is a fundamental parameter in determining intersection capacity and plays a crucial role in optimizing signal timing. Inaccurate estimation of SFR can result in erroneous predictions of vehicle delays, subsequently impacting the assessment of the LOS at signalized intersections. Researchers have emphasized the importance of estimating SFR based on local conditions [5] [6] [43] [44]. Tarko and Tracz [43] highlighted that inaccurate SFR estimations can significantly undermine LOS predictions at signalized intersections, advocating for regularly updated predictive formulas that incorporate local conditions. Similarly, Khatib and Kyte [45] identified errors in input parameters as a major source of bias in LOS predictions, recommending the use of site-specific data. Dowling [44] further demonstrated that local values for parameters such as the peak hour factor (PHF) and SFR substantially reduce errors in delay estimates, particularly when traffic flow exceeds 85% of capacity.

Several U.S.-based studies have explored region-specific SFRs. Cartagena and Tarko [6] examined local base saturation flow rates and lost times at 21 signalized intersections in Indiana, revealing significant variations from the standard HCM value of 1,900 pc/h/ln. Their study proposed a new equation for Indiana's SFR, factoring in town size (based on population) and the number of lanes, elements not considered in the HCM. They found SFRs ranging from 1,352 to 2,178 pc/h/ln, with an average of 1,842 pc/h/ln, and suggested adjustment factors based on town population size. Joseph and Chang [8] conducted a similar

study in Maryland, where SFRs ranged from 1,885 to 2,200 pc/h/ln, recommending a value of 2,080 pc/h/ln for planning purposes. Dunlap's research in Pennsylvania also demonstrated the importance of regional differences, confirming the suitability of a district-wide SFR of 1,800 pc/h/ln, with localized adjustments for individual counties [10]. His study also explored the impact of rain, though the results were inconclusive.

McMahon et al. [28] investigated SFR in five South Florida counties, finding mean values as high as 2,130 pc/h/ln at some intersections, while Bonneson et al. [9] recommended a base SFR of 1,950 pc/h/ln for intersections in Florida, accounting for factors such as right turns and number of lanes. Their study emphasized the need for adjustment factors based on local traffic and geometric conditions.

Internationally, several studies have further highlighted the variability in SFR due to local conditions. Shao et al. [31] in China recommended a base SFR of 1,800 pc/h/ln, accounting for lane width and turn radius, which particularly impacted left-turn lanes. In Doha, Qatar, Hamad and Abuhamda [46] reported a significantly higher SFR of 2,323 pc/h/ln compared to the HCM default. Al-Mistarehi et al. [32] in Jordan estimated a base SFR of 1,720 pc/h/ln, while Al-Omari and Musa [38] in Kuwait analyzed 31 signalized intersections and estimated an SFR of 2,097 pc/h/ln. In South Africa, Bester and Meyers [29] studied intersections in the Stellenbosch area and recommended a base SFR of 2,076 pc/h/ln. In Makkah, Saudi Arabia, Alam et al. [47] reported a much higher SFR of 2,500 pc/h/ln under ideal conditions. Rahman et al. [48] examined SFR in Yokohama, Japan, and Dhaka, Bangladesh, finding SFRs ranging from 1,636 to 2,093 pc/h/ln in Yokohama and 2,006 to 2,091 pc/h/ln in Dhaka, demonstrating that the HCM's default value can overestimate SFR by up to 4.38% in some cases.

The variations in SFR values across both U.S. and international studies highlight the importance of region-specific estimates. Figures 4 and 5 illustrate the comparison between the default SFR value provided by the HCM and the values recommended by researchers across various states in the U.S. and other countries. These figures visually demonstrate the significant discrepancies between the national average and region-specific SFR values.

Figure 4. Comparison among recommended SFR values (in U.S.) versus default HCM value
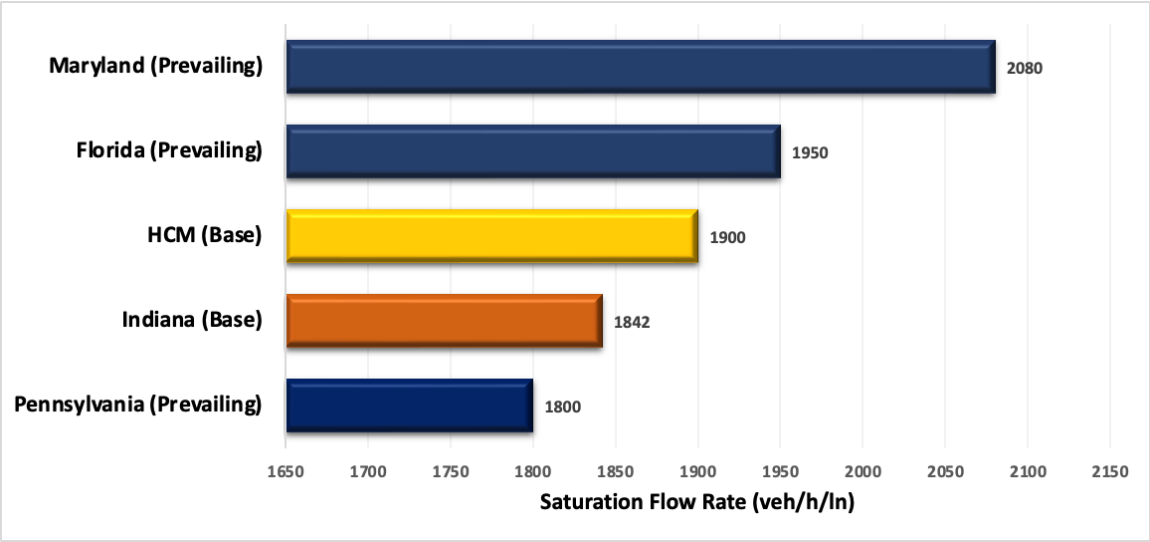
Figure 5. **Comparison among recommended SFR values (global) versus default HCM value**
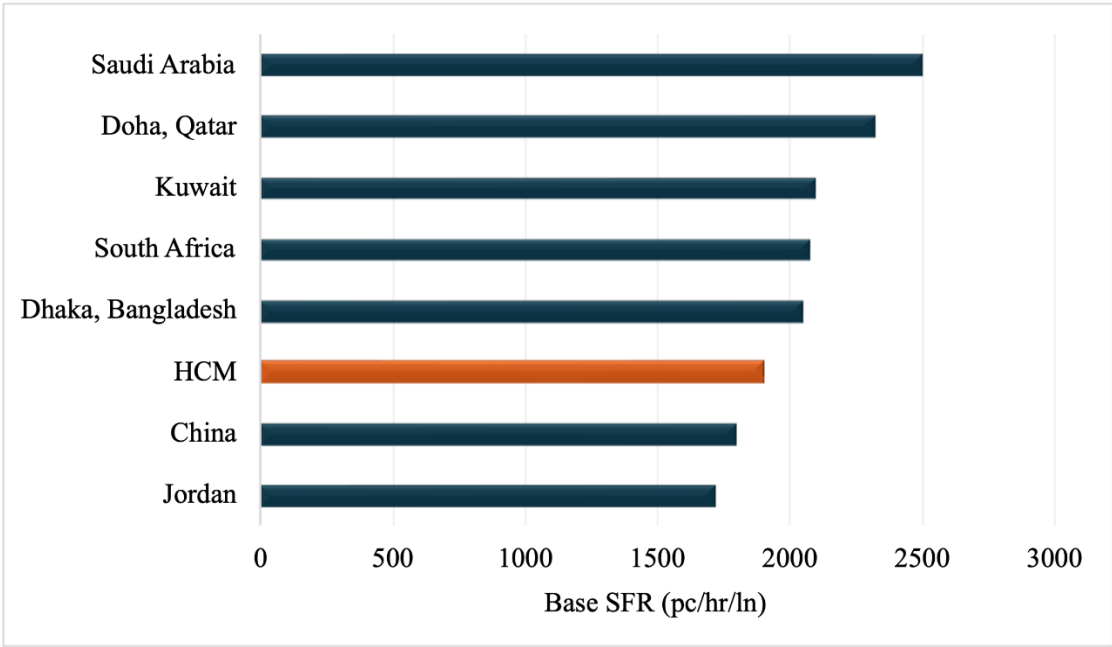
Stop-Controlled Intersections

Critical headway (CH) and follow-up headway (FH) are two fundamental parameters in evaluating the operational performance and capacity of stop-controlled intersections. Various researchers have defined critical headway differently. Troutbeck [49] defined it as the

minimum time interval in the major-street traffic stream that enables a vehicle from the minor street to enter the intersection. In contrast, Raff's definition [50] characterizes the critical gap as the point where the number of accepted gaps shorter than it equals the number of rejected gaps longer than it. Other researchers define it as the gap corresponding to a 50% probability of acceptance or rejection by drivers [51] [52] [53] [54] [55].

Follow-up headway, as defined in the HCM [11], refers to the time between the departure of one vehicle from the minor street and the departure of the next vehicle using the same major-street headway, under continuous queuing conditions on the minor street. Both parameters are essential inputs in gap acceptance models, which are widely used to estimate the capacity of stop-controlled intersections. As such, the accuracy of critical and follow-up headway estimates directly influences the reliability of capacity assessments [56].

However, accurately measuring critical headway is challenging, as it is not directly observable and can vary significantly among drivers based on individual behavior, vehicle type, and situational factors [57]. The HCM provides default values for these parameters, with critical headway ranging from 4.1 to 7.3 sec. and follow-up headway from 2.2 to 4 sec., depending on the roadway configuration and movement type. Nonetheless, the HCM notes that these values represent national averages and may not adequately reflect local conditions. Therefore, estimating location-specific critical and follow-up headways through gap acceptance analysis is essential for accurate capacity evaluation at stop-controlled intersections.

Methodologies for Critical Headway Estimation

Researchers have developed various methods to estimate critical and follow-up headways at stop-controlled intersections, each with its own assumptions, data requirements, and application contexts. These methods aim to capture the decision-making behavior of drivers as they accept or reject gaps in the major-street traffic stream. The fundamental concepts of several widely used methods are discussed below.

Greenshields's method. Greenshields [58] introduced a method for estimating critical headway grounded in traffic flow principles and gap acceptance theory. This approach utilizes a histogram to display the distribution of accepted and rejected gaps by minor road drivers across various gap size intervals. In the histogram, the vertical axis represents the number of gaps, accepted as positive values and rejected as negative values, while the horizontal axis denotes the gap size in seconds. The critical gap is estimated as the mean of the gap interval where the number of accepted and rejected gaps is equal; see Figure 6. While

this method provides a simple and intuitive graphical interpretation of gap acceptance behavior, later studies [59] [60] have noted that small sample sizes can compromise the accuracy of the estimates and potentially distort the resulting critical headway values.

Figure 6. Critical headway estimation by Greenshields's method
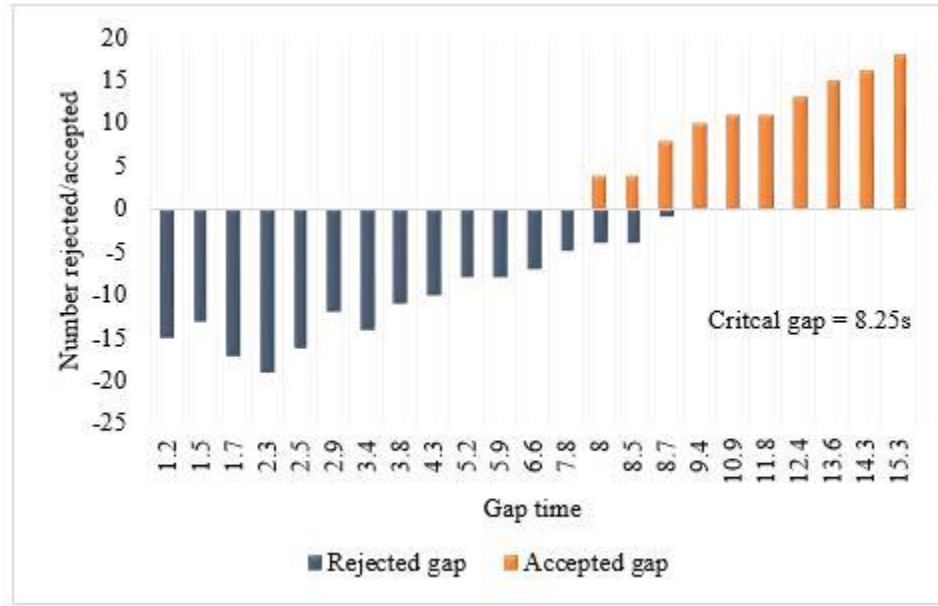
Raff method. The Raff method [50] is one of the earliest and most widely used techniques for estimating critical headway, favored for its simplicity and ease of implementation. In its original formulation by Raff and Hart, the method focuses exclusively on lag data, defined as the time interval between the arrival of a major street vehicle and the arrival of a minor street vehicle at the intersection. The critical lag (L) is defined as the lag value at which the number of accepted lags shorter than L equals the number of rejected lags longer than L.

Despite its widespread use, the Raff method has been critiqued for statistical inefficiency, as it excludes gap acceptance and rejection data, potentially leading to biased results [61] [62]. To address this limitation, Fitzpatrick [12] proposed an enhancement by incorporating both gap and lag data, arguing that there is no meaningful statistical distinction between the two. Further, Miller [61] demonstrated that the Raff method can introduce systematic bias, particularly under varying flow conditions in the major traffic stream.

To estimate the critical gap using the Raff method, the critical gap is determined by employing the empirical distribution functions of accepted gaps, $F_a(t)$, and rejected gaps, $F_r(t)$; see Equation 3.

$$F_a(t) = 1 - F_r(t) \tag{3}$$

Maximum likelihood method. Troutbeck developed a method for estimating critical gap using the MLM, a statistically robust approach grounded in probability theory [49]. This method operates on the principle that a driver's critical gap lies between the largest rejected gap and the accepted gap that immediately follows. By analyzing these observed gap sequences, the method calculates the likelihood that the true critical gap for a driver falls within this range.

To implement the model, a cumulative distribution function (CDF) representing the distribution of critical gaps across the driver population must be specified. Commonly used distributions include the log-normal and Pearson distributions. A key assumption in this approach is that all drivers exhibit consistent behavior, meaning each driver is assumed to have a constant critical gap value during the observation period [63].

This method is widely regarded as highly reliable due to its statistical rigor and ability to utilize both accepted and rejected gap data [63]. It has been adopted by major transportation agencies for estimating gap acceptance parameters and informing design and operational guidelines at unsignalized intersections [64] [65].

Logit method. The logit method is a weighted linear regression model commonly used to estimate the critical gap, particularly when the error variance is either fully known or known up to a proportional constant [59]. This method models the probability of gap acceptance as a function of the gap size and applies the logistic regression framework to estimate the parameters of interest.

$$P = \frac{1}{1 + e^{-(\beta_0 + \beta_1 x)}} \tag{4}$$

where,

P = probability of accepting a gap;

β_0, β_1 = regression coefficients; and

x = variable related to gap acceptance decision.

The logit function can be transferred into a linear equation.

$$P' = \ln\left(\frac{P}{1 - P}\right) = \beta_0 + \beta_1 x \tag{5}$$

where,

P' = transformed probability.

The critical is x- value obtained by substituting P with 0.5.

Siegloch's method. Siegloch's method estimates the critical gap by utilizing the size of the major stream gap and the number of minor street vehicles accepting each major street gap during periods of continuous queuing. The mean values are plotted, with gap size in seconds on the horizontal axis and the number of gap acceptances on the vertical axis. A regression line is fitted to these points, which is then used to calculate the critical gap and follow-up time. For this method to be applicable, the minor road should be saturated with queued traffic [59].

Probability equilibrium method. The probability equilibrium method, introduced by Ning Wu [66], is based on the probability equilibrium between the accepted and rejected gaps. Unlike other methods, it does not require a predefined distribution function for critical gaps or assumptions regarding driver homogeneity and consistency. Additionally, this approach yields a true average of critical headway. Further, it produces an empirical distribution of critical gaps, which is particularly useful for microscopic traffic simulations [66].

Ashworth's method. This method assumes that major stream gaps follow an exponential distribution with statistical independence between consecutive gaps, while the accepted gaps and the average critical gap follow normal distributions. The average critical gap can be estimated using the mean and standard deviation of the accepted gaps, as expressed by the following equation:

$$t_c = \mu_a - P.\sigma_a^2 \tag{6}$$

where,

t_c = average critical gap;
μ_a = mean of accepted gaps (in seconds);
σ_a = standard deviation of accepted gaps; and
P = major stream traffic volume.

Methodologies for Follow-up Headway Estimation

Direct measurement method. Follow-up headway can be directly measured by analyzing time intervals between successive vehicles during periods of continuous queuing at a stop-controlled intersection [57]. This method involves observing and recording the departure

times of vehicles as they pass a designated observation point, either through video footage or manual timing. The follow-up headway is then calculated as the time difference between the departure of one vehicle and the departure of the next vehicle utilizing the same accepted gap in the major traffic stream. This approach provides a straightforward and reliable means of estimating follow-up headway, particularly under stable queue discharge conditions.

HCM method. The HCM provides a base follow-up headway value for stop-controlled intersections, which serves as the foundation for calculating the follow-up headway for specific minor street movements. This base value is then adjusted to account for factors such as the presence of heavy vehicles and the geometric characteristics of the major street.

$$t_{f,x} = t_{f,base} + t_{f,HV} P_{HV} \tag{7}$$

where,

$t_{f,x}$ = follow-up headway for movement x (s);

$t_{f,base}$ = base follow-up headway;

$t_{f,HV}$ = adjustment factor for heavy vehicles (0.9 for major streets with one lane in each direction; 1.0 for major streets with two or three lanes in each direction); and

P_{HV} = proportion of heavy vehicles for movement (expressed as a decimal).

Comparison of Gap Acceptance Methods in Estimating Critical Gaps at Stop-Controlled Intersections

Kay Fitzpatrick [12] conducted a study in Pennsylvania to determine gap acceptance values for truck and passenger car drivers at stop-controlled intersections. The study employed three methods: Greenshields's method, Raff's method, and the Logit method. Among these, the researcher favored the Logit model over the others. Greenshields's method, which evaluates the gap accepted at isolated times without considering the number of gaps accepted or rejected at other time intervals, was found to yield questionable results, particularly when applied to limited data. Similarly, Raff's method, which accounts for cumulative distributions, was deemed less reliable due to its sensitivity to larger gaps. In contrast, the Logit method, which estimates the probability of accepting gaps of different sizes, provided a more accurate estimation of critical gap values.

Kyte et al. [57] expanded on gap-acceptance studies in the United States by estimating critical headway and follow-up headway using the Siegloch method and maximum likelihood estimation. The findings indicated that the maximum likelihood method provided more stable and consistent estimates of critical headway compared to the Siegloch method. When

comparing the estimated critical headway values with the default values provided in the HCM, it was observed that, for lower-speed sites, the HCM critical headway values were consistent with those estimated by the Siegloch method. However, the maximum likelihood method produced values that were equal to or lower than the HCM values. For higher-speed sites, the HCM values were approximately 2 sec. higher than those estimated by both methods. Additionally, follow-up headway was measured using both the Siegloch method and direct field observation, with findings showing some consistency between these two approaches. When compared to the HCM's default follow-up headway values, the study found consistency among the HCM values, Siegloch estimates, and direct measurements.

Further comparative analysis by Troutbeck [67] examined the maximum likelihood method and the probability equilibrium method (PEM) for estimating critical gaps at unsignalized intersections, considering varying traffic conditions and driver behaviors. The study found that the maximum likelihood method consistently produced accurate and unbiased estimates of both the mean and standard deviation of critical gaps, even in cases where driver behavior was inconsistent. In contrast, the probability equilibrium method demonstrated a notable bias, particularly influenced by the flow in the priority stream, and tended to underestimate the variance of critical gaps.

In a separate study, Troutbeck [68] examined the estimation of critical gaps for both vehicle and pedestrian movements at unsignalized intersections, comparing the Raff method, the revised Raff method, and the maximum likelihood method. The study concluded that the maximum likelihood method was the preferred technique due to its superior performance in estimating the mean critical gaps. However, the modified Raff method, which incorporates the maximum rejected gap, was identified as an acceptable alternative when the maximum likelihood method is not feasible.

In their study, Brinol et al. [63] reviewed several methods for estimating critical gaps at unsignalized intersections, assessing their effectiveness based on criteria such as consistency, robustness, and compatibility with capacity models. The study found that the maximum likelihood method and Hewitt's method provided the most reliable and consistent estimates of critical gaps, even under varying traffic conditions. These methods were independent of the traffic volume on the major street, making them particularly suitable for practical applications. In contrast, Ashworth's and Raff's methods exhibited significant bias and sensitivity to traffic volumes, reducing their reliability. Siegloch's method performed well in saturated traffic conditions but showed limitations when applied to more realistic, non-Poisson traffic scenarios.

A.J. Miller's [61] comparative study of nine gap-acceptance methods focused on efficiency and bias, as well as offering recommendations for practical use. The study found that five of the methods exhibited significant bias and should not be recommended without the application of bias corrections. The Ashworth method demonstrated moderate efficiency but was only recommended in situations where the gaps offered were not highly correlated. In contrast, the maximum likelihood method consistently produced satisfactory results across various datasets and emerged as a strong candidate for practical applications in estimating critical gaps.

McGowen and Stanly [69] proposed a new gap-acceptance model requiring only accepted or rejected gaps and produced unbiased estimates. The study concluded that, while the Troutbeck method is widely accepted, it can result in biased outcomes and is less effective when applied to datasets containing only rejected gaps. In contrast, the proposed alternative method is preferred for its flexibility and ability to yield unbiased results, particularly in cases where only rejected gap data are available. However, the accuracy of this method is contingent on the correct estimation of traffic flow on the major street.

Pawar and Patil [70] analyzed spatial critical gaps at high- and medium-speed two-way stop-controlled (TWSC) intersections using both parametric (Binary Logit Model, BLM) and non-parametric (Support Vector Machines, SVM) techniques. The study found that both BLM and SVM provided reliable estimates for spatial critical gaps. However, SVM demonstrated significant potential as an alternative to BLM, producing similar estimates with slight variations, especially at high-speed intersections, highlighting its viability for such applications.

Mohan and Chandra [71] proposed a novel approach, the Occupancy Time Method (OTM), for estimating critical gaps at two-way stop-controlled intersections under heterogeneous traffic conditions, using occupancy time data. They compared this method with several established techniques, including the MLM, Modified Raff Method, Harders's Method, Logit Method, Probability Equilibrium Method (PEM), and Lag Method. Their findings indicated that traditional methods like MLM and the Modified Raff Method were inadequate for addressing the complexities of heterogeneous traffic in India, often resulting in unrealistically low critical gap estimates. In contrast, the OTM method outperformed both MLM and the Modified Raff Method by better capturing the intricate driver behavior and vehicle movements typical of such intersections. OTM was preferred for its closer alignment with actual field conditions, while MLM tended to overestimate capacity and the Modified Raff Method underestimated it.

In summary, several researchers have compared multiple gap-acceptance methods across different contexts, favoring certain techniques for their reliability and accuracy. Table 4 provides a concise comparison of the methods analyzed in the studies and the preferred methods identified by the researchers.

Table 4. Summary of methods compared and preferred methods in previous gap-acceptance studies

Researcher(s)	Methods Compared	Preferred Method	Reason for Preference
Kay Fitzpatrick [12]	Greenshield, Raff, Logit	Logit	More accurate estimation of critical gap values
Kyte et al. [57]	Siegloch, Maximum Likelihood	Maximum Likelihood	More stable estimates of critical headway
Troutbeck [67]	Maximum Likelihood, Probability Equilibrium (PEM)	Maximum Likelihood	Accurate and unbiased estimates under all conditions
Troutbeck [68]	Raff, Modified Raff, Maximum Likelihood	Maximum Likelihood	Superior performance in estimating mean critical gaps
Brinol et al. [63]	Maximum Likelihood, Hewitt, Ashworth, Raff, Siegloch	Maximum Likelihood, Hewitt	Consistency, independence from major street traffic volume
A.J. Miller [61]	Nine methods, including Ashworth and Maximum Likelihood	Maximum Likelihood	Consistently reliable across datasets
McGowen & Stanly [69]	Troutbeck, New Model	New Model	Flexibility and unbiased results with rejected gaps
Pawar & Patil [70]	Binary Logit, Support Vector Machines (SVM)	Support Vector Machines (SVM)	More reliable at high-speed intersections
Mohan & Chandra [71]	Maximum Likelihood, Modified Raff, Occupancy Time	Occupancy Time Method (OTM)	Better performance under heterogeneous traffic conditions

Factors Affecting Critical Headway and Follow-up Headway

At stop-controlled intersections, drivers on the minor approach are required to stop and evaluate gaps in the major street traffic stream before proceeding. This gap acceptance process is dynamic and influenced by a complex interaction of driver behavior, roadway characteristics, and environmental conditions. Previous studies have identified key factors, such as intersection geometry, driver characteristics, and vehicle type, that significantly influence both critical headway and follow-up headway. This section reviews findings from

the literature to better understand how these factors impact driver decision-making and capacity estimation at unsignalized intersections.

As major street traffic volume increases, minor street drivers experience greater difficulty in identifying acceptable gaps, often resulting in shorter accepted gaps. Kyte et al. [72] reported a notable decline in accepted gap size once the major street volume exceeds 90 vehicles per hr. Similarly, minor street traffic volume contributes to shorter critical headways due to longer queues and increased pressure to proceed. Tupper et al. [73] found that the presence of a queue reduced estimated critical headways by approximately 1.5 sec., attributing this to social pressure from trailing vehicles. Additionally, drivers who reject multiple gaps before accepting one tend to eventually accept gaps that are 2–3 sec. shorter [73]. This behavior is further influenced by prolonged waiting times, which can lead drivers to prioritize reduced delay over safety [72].

The presence of passengers also impacts gap acceptance, especially among young drivers, who may accept gaps 1 to 1.5 sec. shorter due to peer pressure or distraction [73]. Driver age and sex have also been shown to affect gap acceptance behavior. Studies indicate that male drivers accept gaps 0.5 to 1.5 sec. shorter than female drivers, while younger drivers accept significantly shorter critical gaps, by as much as 1 sec., compared to adults [73]. The difference between adult and elderly drivers is less pronounced [73], although older drivers generally accept longer gaps than both teenagers and adults [52].

Temporal factors, such as time of day and lighting conditions, also influence gap acceptance. Drivers are more likely to accept shorter gaps during daytime than at night [52]. Additionally, more aggressive behavior is observed during morning and evening peak periods compared to midday, likely due to higher traffic volumes and commuting time constraints [73].

Intersection geometry, vehicle type, and maneuver type further affect critical headways. Left-turning vehicles typically require larger gaps than through vehicles, which in turn need larger gaps than right-turning vehicles [72]. Tian et al. found that smaller turn angles facilitate easier maneuvers, resulting in critical gaps that are approximately 1 sec. shorter than those for larger angles [74]. Increases in the number of lanes on the major street and the number of legs at the intersection contribute to greater maneuver complexity and therefore larger critical gaps. Additionally, critical headways increase with approach grade [74].

Vehicle type is another influential factor. Heavy vehicles require larger critical gaps and longer follow-up times due to slower acceleration. Tian et al. reported that heavy vehicles need critical gaps approximately 1 sec. longer than passenger cars, with follow-up headways

also increased by a similar margin [74]. Mohan et al. found that two-wheelers had the smallest critical gaps, while trucks required the largest [71]. The proportion of large vehicles in the major stream also affects gap acceptance, as drivers are generally more hesitant to accept gaps involving larger conflicting vehicles, whereas smaller or mid-sized vehicles have less influence on the decision.

While the HCM incorporates some of these factors into its procedures for estimating critical and follow-up headways, not all of the variables discussed above are explicitly considered. Table 5 summarizes key variables identified in the literature that significantly impact headway values but are not currently included in the HCM framework.

Table 5. Consideration of critical and follow-up headway influencing factors

Factors	HCM	Studies
Traffic Flow on Major Street	✓	[72]
Traffic Volume on Minor Road	✓	[73]
Presence of Queues		[72], [73]
Passenger Presence		[73]
Driver Age and Sex		[52], [73]
Time of Day		[52], [73]
Maneuver Direction	✓	[57], [72]
Turn Angle		[74]
Vehicle Type	✓	[71], [74]
Number of Lanes and Legs	✓	[74]
Approach Grade	✓	[74]

Objective

The primary objectives of this research project were to:

- Estimate the saturation flow rate (SFR) for selected signalized intersections, and
- Analyze critical headway (CH) and follow-up headway (FH) on stop-controlled intersections.

Scope

The statewide data collected for this research utilized intersection traffic flow data from available sources, including 511 video data provided by the state and intersections selected by District Engineers. The final data analysis was compiled by combining these sources, focusing on intersections with sufficient sample sizes for analysis. This process resulted in 51 signalized four-leg intersections and 26 four-leg two-way stop-controlled intersections across a total of eight districts in Louisiana.

Methodology

This section outlines the methodology used to estimate the HCM parameters for Louisiana. A generalized multi-step process was conducted to achieve this objective; see Figure 7. Initially, suitable methods for estimating intersection capacity parameters were selected, considering Louisiana's traffic conditions. Next, a list of signalized and stop-controlled intersections was prepared based on predefined criteria, which was subsequently used for data collection and database preparation for analysis. Using this database, the intersection capacity parameters (SFR, CH, and FH) were estimated, and the factors influencing these parameters were identified. Each of these steps is discussed in detail in the following sections.

Figure 7. Multi-step process of HCM parameter estimation
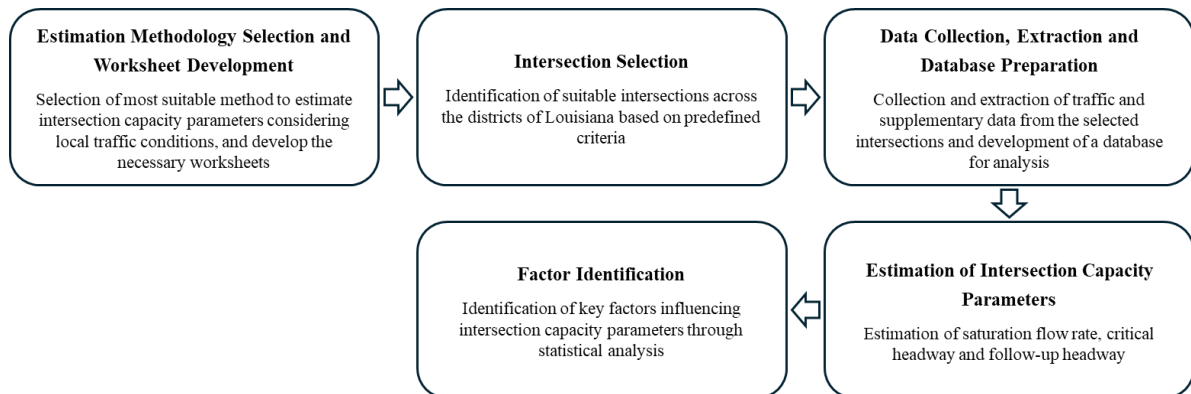
Intersection Selection

The process of identifying suitable intersections began with the statewide travel information website (511la.org) to evaluate camera accessibility. The 511 system includes 296 CCTV cameras covering major signalized intersections across Louisiana's highways, primarily on higher functional classification roadways. However, the system does not cover stop-controlled intersections, and some camera views were unusable due to poor angles or adverse weather conditions. Therefore, intersections covered by the 511 system that met the selection criteria and had usable footage were included in the study.

Additionally, a limited number of state-controlled intersections with cameras operated by the Louisiana Department of Transportation and Development (DOTD) were identified. These included 23 signalized intersections and 2 two-way stop-controlled intersections, which were evaluated using the same criteria.

To expand the sample, representatives from Louisiana DOTD in various districts were contacted to obtain a list of strategically important intersections not covered by the 511 system. Further, the annual crash database developed and maintained by Louisiana DOTD was used to identify additional intersections. The highway section table from this Microsoft Access database was filtered to select TWSC intersections with higher AADT on minor roads. Intersections from this combined list that met the predefined criteria were included in the study.

A representative sample of intersections for analysis was developed by establishing specific selection criteria for both signalized and stop-controlled intersections. The primary objective of the selection process was to ensure that the chosen intersections reflected a diverse range of functional classifications, lane configurations, and area types. Priority was given to intersections with accessible camera coverage to facilitate accurate data collection. Figure 8 shows all the sources used in intersection selection process. For consistency, the initial key selection criteria are outlined below:

Signalized intersection selection criteria:

- Sufficient traffic flow with a minimum of seven vehicles during the red phase to allow for SFR estimation, preferably at intersections with higher annual average daily traffic (AADT).

- At least one clearly visible lane dedicated to through traffic, with separate analyses for intersections with and without turning lanes.

- Only four-legged intersections were considered.

- Avoidance of intersections with high truck percentages or significant lane utilization issues (e.g., bus stops, parallel parking, railroad tracks).

Stop-controlled intersection selection criteria:

- Only four-legged two-way stop-controlled (TWSC) intersections were considered.

- Prioritize intersections with higher AADT on the minor road to ensure sufficient sample size.

- Avoidance of intersections with high truck percentages or significant lane utilization issues (e.g., bus stops, parallel parking, railroad tracks).

Figure 8. Sources of intersection selection approach

511la.org Camera
296 Cameras covering major signalized Intersections across Louisiana's highways

DOTD Crash Database
Highway section table – TWSC intersection with high AADT on the minor street

DOTD Representative
Contacted to collect lists of intersections
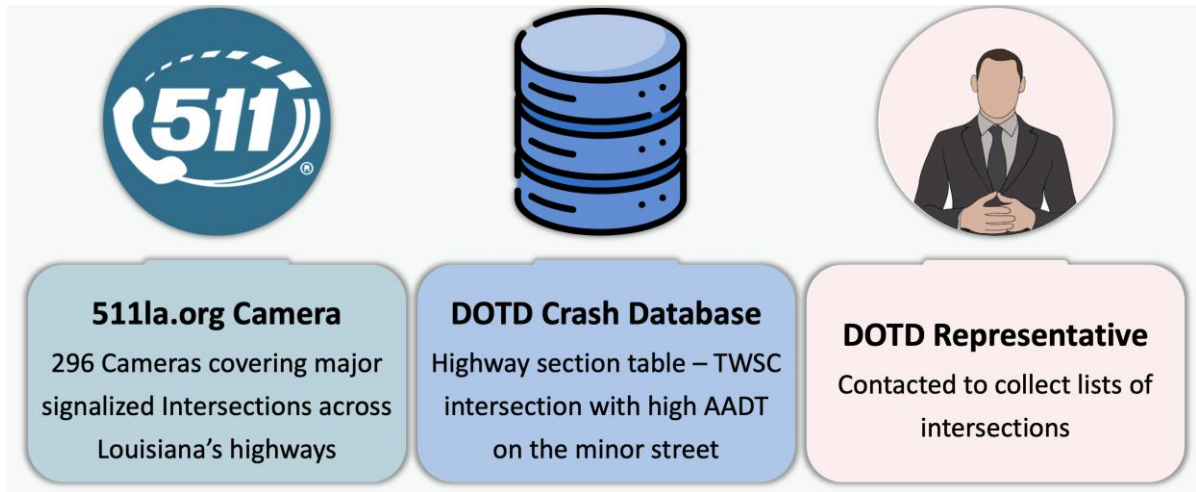
Supplementary tools, such as Google Earth Street View and Louisiana DOTD's pavement management data repository, iVision, were used to gather geometric information and categorize intersection geometry features. After applying the criteria and reviewing the available data, a total of 75 intersections were selected for the study, including 49 signalized intersections and 26 stop-controlled intersections. Figures 9 and 10 illustrate the distribution of the signalized and stop-controlled intersections considered for this study. Data were not available for District 58, and no intersection in 511 existed at the time of data collection.

Figure 9. Distribution of signalized intersections across districts of Louisiana
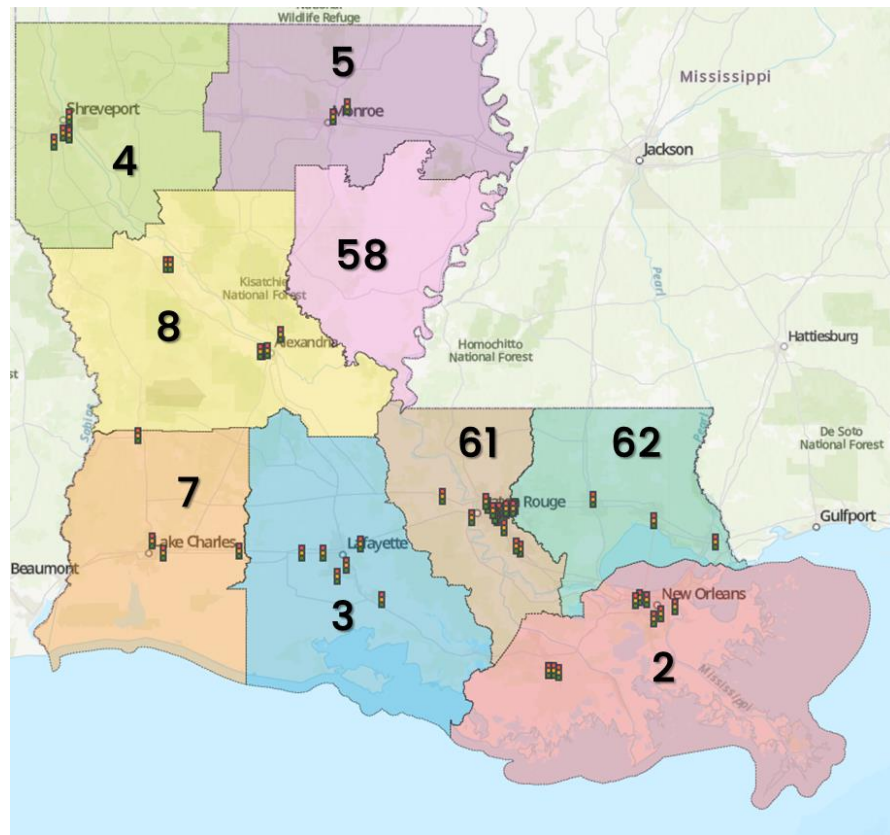
Figure 10. Distribution of stop-controlled intersections across districts of Louisiana
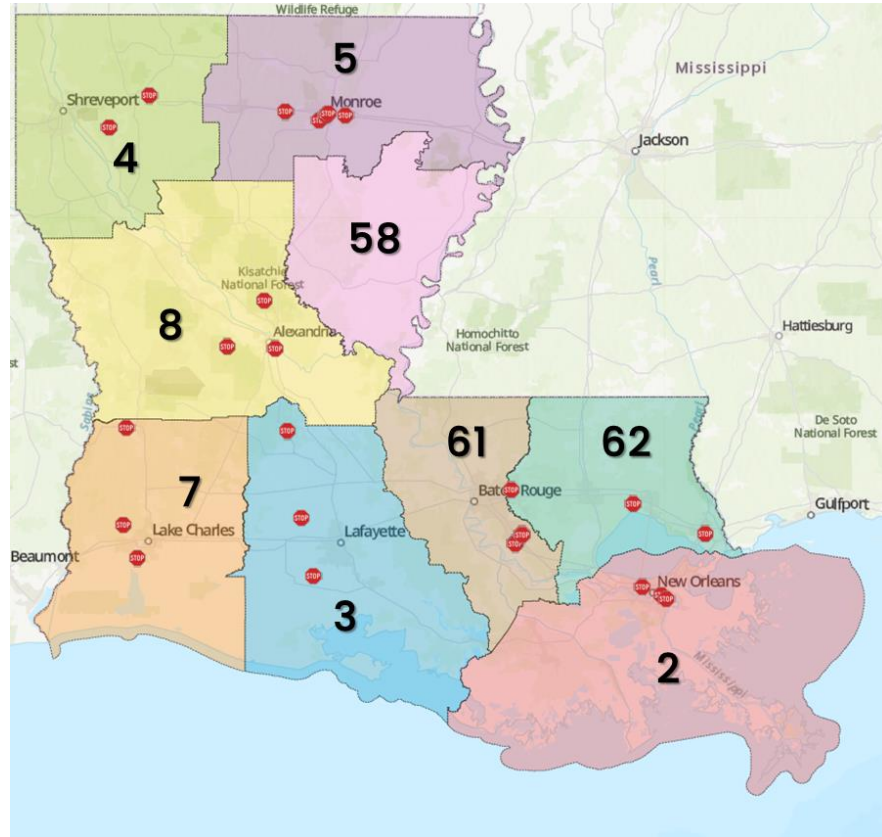
Selected Methods to Estimate Parameters

Based on a review of existing literature, and considering the advantages and limitations of each method as well as Louisiana's traffic conditions, the most suitable methods were selected for this study. For estimating the SFR at signalized intersections, the Saturation Headway/Field Estimation method was selected. The Maximum Likelihood Estimation (MLE) method was chosen for estimating CH at stop-controlled intersections, while the Direct Measurement method was selected for estimating FH at stop-controlled intersections. These methodologies are described below.

Saturation Headway Method of Estimating SFR at Signalized Intersections

The Saturation Headway/Field Measurement method of estimating SFR, as described in the HCM, calculates the SFR by taking the reciprocal of the saturation headway.

This method was selected for this study because it allows for detailed, accurate, and site-specific estimation of SFR. Saturation headway refers to the average time gap between vehicles that occurs after the fourth vehicle in the queue, continuing until the last vehicle in the initial queue clears the signalized intersection; see Figure 11 [11]. This method involves directly measuring traffic flow during the green phase at a specific intersection. To ensure an accurate estimation of SFR, which reflects the true capacity of the intersection while excluding the effects of initial startup delays and ensuring stabilized traffic flow, time recording began when the rear axle of the fourth vehicle in the queue (which was stationary while waiting for the green signal) crossed the stop line. The recording ended when the rear axle of the seventh, eighth, ninth, or tenth vehicle (depending on which was the last vehicle in the stopped queue when the green signal was given) crossed the stop line.

Figure 11. Saturation headways at signalized intersections [11]
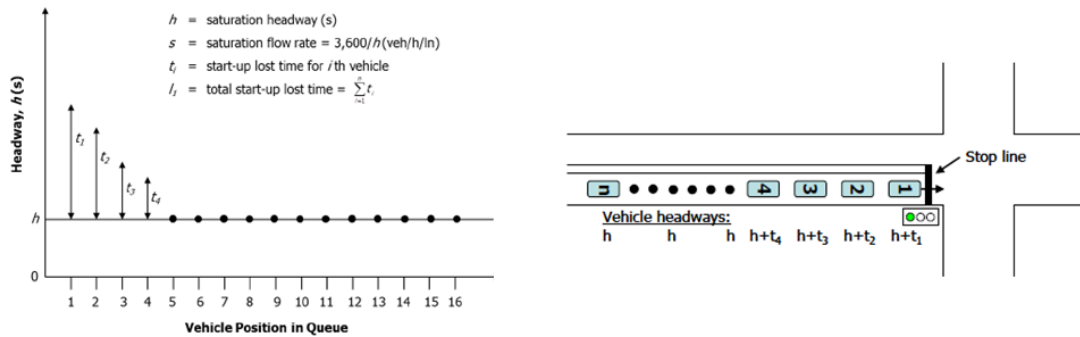
During this study, in cases where the stop line was not visible, a consistent alternative reference line was established just beyond the typical stopping position of the first queued vehicles. Additionally, the developed worksheet (Figure 12) recorded data on the number of heavy vehicles, left- and right- turning vehicles, and weather and pavement conditions during the data collection period, ensuring comprehensive documentation of factors influencing the SFR.

Figure 12. SFR estimation worksheet

Saturation Flow Rate Estiamtion Worksheet												
North/South							District					
East/West							Parish					
Approach Studied							Int. ID					
Weather							Time					
Pavement Condition							Date					

Cycle	Elapsed time 1 (sec)	Total # vehicles	Elapsed time 2 (sec)	Total # vehicles	Elapsed time 3 (sec)	Total # vehicles	# Heavy vehicle	# R/L turn vehicles	Calc SFR 1	Calc SFR 2	Calc SFR 3	Avg. SFR
1												
2												
3												
4												
5												
6												
7												
8												
9												
10												
11												
12												
13												
14												
15												
16												
17												
18												
19												
20												

The saturation headway was calculated using the following equation:

$$h_s = \frac{t}{n} \tag{8}$$

where,

h_s = saturation headway (sec.);

t = elapsed time (sec.); and

n = total number of vehicles passing.

The saturation flow rate was then calculated by dividing 3,600 by saturation headway, as presented in Equation 2.

To minimize human error, SFR was calculated three times for each signal cycle, and the average of these calculations was taken. For each intersection, at least 15 and up to 20 signal cycles were measured, and the average of these cycles was used as the estimated SFR for that specific intersection.

After computing the prevailing SFR at each study intersection, the adjusted saturation flow rate ($SFR_{adjusted}$) was estimated by applying the adjustment factors outlined in the HCM. This involved adjusting the base saturation flow rate of 1,900 (pc/h/ln) to account for lane width, heavy vehicle presence, approach grade, and turning movements. Other adjustment factors, such as those related to work zones, pedestrian or bicycle activity, and bus stops, were assigned a value of 1.0, as the study intersections were unaffected by these elements. Specifically, there were no work zones, no pedestrian or bicycle crossings, and no bus stop activities during the data collection period.

For study approaches with only through movements, the adjusted saturation flow rate was calculated using the following equation:

$$SFR_{adjusted,th} = S_o * f_w * f_{HVg} \tag{9}$$

where,
SFR_o = base SFR (1,900 pc/h/ln);
f_w = adjustment factor for lane width; and
f_{HVg} = adjustment factor for heavy vehicle and approach grade.

For intersections where the study approach included turning movements on shared lanes, the initially adjusted through-lane saturation flow rate ($SFR_{adjusted,th}$) was further adjusted based on the type of turning movement observed.

For approaches where right-turning movements occurred on shared lanes, the adjusted SFR was calculated using the permitted right-turn adjustment formula:

$$SFR_{sr} = \frac{S_{adjusted,th}}{1 + P_R(\frac{E_R}{f_{Rpb}} - 1)} \tag{10}$$

where,
SFR_{sr} = saturation flow rate in shared right-turn and through lane with permitted operation (pc/h/ln);
$S_{adjusted,th}$ = saturation flow rate of an exclusive through lane;
P_R = proportion of right-turning vehicles in the shared lane (decimal);
E_R = equivalent number of through cars for the protected right-turning vehicle = 1.18; and
f_{Rpb} = pedestrian-bicycle adjustment factor for right-turn group (=1 in this study).

For left-turning movements on shared lanes, the adjusted SFR was calculated using the following equation. Given that the pedestrian/bicycle adjustment factor is f_{Lpb} =1 for all study intersections, the equation simplifies as:

$$SFR_{sl} = \frac{S_{adjusted,th}}{1 + P_L(E_R - 1)} \qquad (11)$$

Finally, the local base SFR for each intersection was computed using the ratio of the prevailing SFR to the adjusted SFR, scaled by the base SFR value:

$$SFR_{base} = 1900 * \frac{S_{prevailing}}{S_{adjusted}} \qquad (12)$$

MLE Method of Critical Headway at Stop-Controlled Intersections

CH and FH for stop-controlled intersections were estimated using gap acceptance analysis. According to previous studies, the MLE method provides accurate, unbiased, and stable results, even with small sample sizes [57] [61] [75] [76] [77]. Given the low traffic volumes at most stop-controlled intersections in Louisiana and the demonstrated robustness of the MLE method, it was selected for CH estimation in this study.

The MLE method assumes that a driver's critical gap is greater than the largest gap they rejected and smaller than their accepted gap. Troutbeck (1992) modeled the probabilistic distribution of critical gaps using a log-normal distribution, which is characterized by right skewness and non-negative values, aligning with expected conditions at stop-controlled intersections [49]. The following assumptions are made:

- r_i = the logarithm of the largest gap rejected by the ith driver. r_i = 0 if no gap was rejected;

- a_i = the logarithm of the gap accepted by the ith driver;

- μ = mean of the distribution of the logarithms of the individual drivers' critical gaps;

- σ^2 = variance of the distribution of the logarithms of the individual drivers' critical gaps;

- $f(x)$ = probability density function for the normal distribution; and

- $F(x)$ = cumulative distribution function for the normal distribution.

The maximum likelihood of a sample of n drivers having an accepted gap and a largest rejected gap of (a_i, r_i) is expressed as:

$$\prod_{i=1}^{n} [F(a_i) - F(r_i)] \tag{13}$$

Taking the logarithm of the likelihood function gives:

$$L = \sum_{i=1}^{n} \ln [\, F(a_i) - F(r_i)] \tag{14}$$

Maximizing this likelihood yields estimates for μ and σ^2, which are then used to calculate the mean critical t_c and its variance s^2 using the following equations:

$$t_c = e^{\mu + 0.5\, \sigma^2} \tag{15}$$

$$s^2 = t_c^2 (e^{\sigma^2} - 1) \tag{16}$$

Required data size for MLE method. The iterative nature of the MLE method suggests that a large dataset may be necessary to produce accurate results. In Troutbeck's study [67], the difference between the mean of 100 critical gap estimates and the true critical gap was analyzed under varying major street traffic volumes of 300, 900, and 1,500 vehicles per hour. The results, presented in Figure 13, illustrate the relationship between the number of observed drivers, ranging from 10 to 100, and the accuracy of the estimated mean critical gap.

Figure 13. Required data size for MLE method [67]
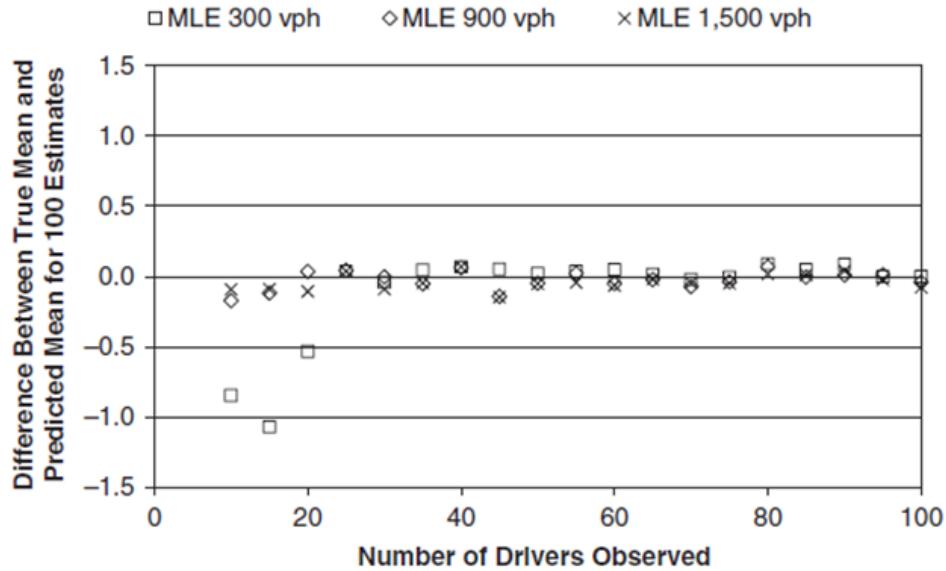
For low traffic volumes and fewer than 20 observed drivers, the estimated mean critical gap deviates significantly from the true value. However, when the number of observed drivers exceeds 25, the estimated mean critical gap closely aligns with the true value, regardless of the major street volume. This demonstrates that the MLE method provides an unbiased estimate when sufficient data is available. Based on these findings, a minimum of 25 to 30 observed drivers is recommended for reliable critical gap estimation using the MLE method [67].

Further, potential biases can arise from minor road drivers who accept gaps in the major street flow without rejecting any. Excluding these cases from the dataset could introduce bias into the results. To mitigate this issue, the recommended approach is to assign a maximum rejected gap of zero or a small value when no gaps are explicitly rejected, ensuring the data remains representative and unbiased.

Definition of gap events. Gap events are time intervals that define the beginning and end of gaps in the major street traffic. To apply the MLE method, it is essential to identify both the maximum rejected gap and the accepted gap for the subject minor road vehicle, i.e., the vehicle attempting to merge into the major street traffic. These gap events are determined using the passage times of vehicles in the major street, where a gap is the time interval between the begin gap and end gap events.

A begin gap event is triggered by the passage of a major street vehicle that directly conflicts with the subject vehicle, while an end gap event occurs with the passage of a higher-priority major street vehicle that also conflicts with the subject vehicle. Accurate identification of these conflict points is critical for defining gap events correctly. For example, in the case of a left-turning vehicle on the major street, only through and right-turning vehicles on the opposing major street are considered end gap events. Conversely, for movements originating from the minor street, all major street vehicles are treated as end gap events. Generally, vehicles on the opposing minor street do not exhibit clear priority over the subject vehicle, regardless of their movements.

If the major street comprises multiple lanes, only vehicles in lanes that physically conflict with the movement of the subject vehicle from the minor street are considered in the calculation of gap events. Figure 14 illustrates an example of gap events at a multi-lane intersection, where a left-turning minor street vehicle conflicts with right-bound vehicles in lanes 1 and 2, as well as a left-bound vehicle in lane 1. Consequently, vehicles in these three lanes are included when defining the gap events. This approach ensures a precise understanding of the temporal and spatial dynamics influencing gap acceptance behavior.

Figure 14. Gap events at multi-lane stop-controlled intersections
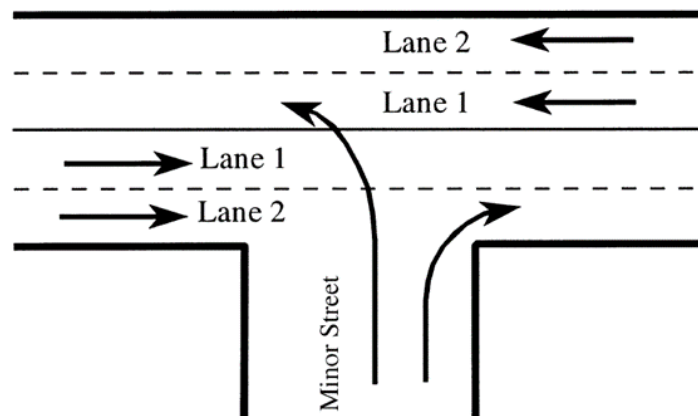
Spreadsheet procedure of the MLE method. The iterative procedure of the MLE method, while seemingly complex, can be effectively implemented using spreadsheet commands. The process begins with initial estimates or guesses for the mean and variance of the critical gap. These initial values are then refined iteratively. Subsequently, the mean (μ) and variance of the log of the critical gap (σ^2) are calculated using the following equations and recorded in Cells D45 and D46 of Table 6.

$$\sigma^2 = \ln\left(\frac{s^2}{m^2} + 1\right) \tag{17}$$

$$\mu = \ln(m) - 0.5\sigma^2 s^2 = t_c^2(e^{\sigma^2} - 1) \tag{18}$$

where,

m is the mean; and

s is the standard deviation of the critical gap.

Assuming a lognormal distribution of critical gaps, the values in Column D of Table 6 were calculated using the following Excel statement:

$$= LN(NORM.DIST(LN(B2), D\$45, D\$46, TRUE) -$$
$$NORM.DIST(LN(C2), D\$45, D\$46, TRUE))$$

Cell D42 contains the formula SUM(D2:D41), which computes the sum of likelihood values for the dataset. Initially, the sum in Cell D42 is −10.42, based on the first estimated or guessed values of the mean (7.0 sec.) and standard deviation (3.0 sec.) for the critical gap.

The Solver tool in Excel, which performs iterative optimization, was used to maximize the logarithm of the likelihood recorded in Cell D42. Through this iterative procedure, the values of the mean and standard deviation converged to 5.399 sec. and 0.8163 sec., respectively. As a result, the sum (logarithm of the likelihood) increased to −4.82. These optimized values for the mean and standard deviation of the critical gap/headway represent the results of the MLE method.

<div align="center">

Table 6. Spreadsheet procedure of MLE method

</div>

	A	B	C	D
1	Driver	Accepted gap, a	Maximum rejected gap, r	$Ln[F(a) - F(r)]$
2	1	10.89	5.39	-0.7502
3	2	10.52	0.1	0.0000
4	3	38.15	2.04	0.0000
5	4	27.58	2.83	0.0000
6	5	7.67	0.1	-0.0079
7	6	8.6	2	-0.0008
…	…	…	…	…
41	40	22.39	4.59	-0.1711
42	Sum			-4.8239
43	Mean critical gap			**5.4**
44	Standard deviation of critical gap			**0.816**
45	Mean of log of critical gap			1.6748
46	Standard deviation of log of critical gap			0.1504

Direct Measurement Method of Estimating FH

The field measurement method was used to estimate the follow-up headway (FH) at stop-controlled intersections. A worksheet was developed to directly estimate FH using video recordings. From the video footage, it was determined whether the following vehicle was queued and whether both the lead and following vehicles utilized the same gap in the conflicting traffic stream. FH was measured as the time difference between the exit-queue times of the lead and following vehicles, using the stop line as a reference point. If the stop line was not visible, a consistent alternative reference line was established to maintain accuracy.

The follow-up times were categorized based on the type of turning movements. Table 7 presents the worksheet used in this analysis, where each row represents vehicles on the minor street that accepted the same gap in the major street. For example, in the initial row of Table 7, the lead vehicle is a car, and the following vehicle is a pickup truck. The follow-up time for the pickup truck is calculated as the difference in exit-queue time between the car and the pickup truck. If an SUV is queued behind the pickup truck and also utilizes the same gap, the follow-up time for the SUV is calculated as the difference between the exit-queue times of the pickup truck (i.e., lead vehicle) and the SUV (i.e., following vehicle).

This iterative process is repeated for each queued vehicle on the minor street that utilizes the same gap within the conflicting traffic stream, thereby computing the FH for each vehicle accordingly.

Table 7. FH estimation worksheet

Sl.	Subject Vehicle Type	Movement	Exit Queue	Queued	Follow-up Headway (sec.)
1	Car	SBLT	15.14.54		
	Pickup	SBLT	15.15.01	Y	7
	SUV	SBRT	15.15.10	Y	9
2	Car	SBLT	15.17.33		
	Pickup	SBRT	15.17.40	Y	7
	SUV	SBRT	15.17.58	Y	4
3	Firetruck	SBLT	15.19.05		
	SUV	SBRT	15.19.10	Y	5
	Car	SBLT	15.19.16	Y	6
4	Car	SBLT	15.19.25	Y	9
	SUV	SBLT	15.19.40		
	Car	SBRT	15.19.44	Y	4
5	SUV	SBRT	15.20.33		
	Pickup	SBRT	15.20.39	Y	6

Video Data from Intersections

Based on the prepared list of the intersections, a comprehensive database for signalized and stop-controlled intersections was developed by integrating data from multiple sources. The process involved real-time traffic data collection, supplemented by relevant geographical attributes (e.g., lane geometry, lane width), operational characteristics (e.g., traffic volume, vehicle classification, pedestrian, and cyclist activity), and additional information (e.g., area type, population density). Video data served as a primary source for traffic analysis, particularly for capacity measurements. Given the study's focus on estimating intersection capacity, data collection prioritized intersections with significant traffic demand for signalized intersections or sufficient vehicle queuing for stop-controlled intersections. To analyze factors influential to observation data for each cycle, data were initially compiled during all visible available hours. To ensure sufficient sample size, data collection was conducted during peak traffic periods—6:00 A.M. to 9:00 A.M. for morning peak and 3:00 P.M. to 6:00 P.M. for evening peak. Additional off-peak observations were also included, with all datasets meeting minimum sample size requirements. The HCM recommends extended data collection periods for planning-level analyses.

For intersections with camera coverage from the 511 system and Louisiana DOTD cameras, video data were obtained by screen-recording live camera feeds. For intersections without

camera coverage, field cameras were installed to capture the required data for analysis; see Figure 15. The study utilized countCAM4, a compact and lightweight traffic counting camera capable of continuous multi-day video recording. A detailed description of countCAM4 is provided in Appendix A. These field cameras were strategically positioned to ensure comprehensive coverage of vehicle movements at the study approaches.

Figure 15. Installed camera at study intersections

For signalized intersections, cameras were generally positioned to monitor the major approaches. However, in cases requiring additional coverage, approaches were selected randomly. For stop-controlled intersections, cameras were positioned to record vehicle queues on minor roads and traffic flow on major roads. When feasible, camera angles were adjusted to capture multiple approaches simultaneously. At intersections where a single camera could not cover all necessary details, multiple cameras were deployed.

Each camera was assigned a unique identification number linked to the intersection and its control type. Video recordings were captured continuously for three consecutive days at each intersection. The recordings were subsequently processed to extract the data required for analysis. Cameras were positioned to record vehicle queues on the intended approach with a queue; see Figure 16 (TWSC) and Figure 17 (signalized intersection).

Figure 16. Camera view at a stop-controlled intersection

Figure 17. Camera view covering multiple approaches

Supplementary Data

Roadway geometry provides essential information about the physical characteristics of a road directly influencing traffic flow, capacity, and safety. Relevant roadway geometry data for this study were collected from Google Earth Pro and Fugro iVision5 to ensure accurate and comprehensive data collection. Traffic volume data at the study intersections were obtained from the Regional Integrated Transportation Information System (RITIS) and the MS2 Traffic Count Database System. Population density data were collected from the United States Census Bureau database. Additional data, such as weather and pavement conditions, vehicle type, number of rejected gaps, and vehicle movement type were collected directly from the video recordings. The data collection process from each source is described below:

Google Earth Pro provides advanced geospatial tools for exploring and analyzing Earth's surface using high-resolution satellite imagery, 3D terrain, and maps. Its features include importing GIS data, measuring distances and areas, creating interactive tours, and exporting high-resolution images and videos. In this study, Google Earth Pro was used to gather information on turning radius, intersection gaps, availability of pedestrian crossings, distance of access points from intersections, and speed limits. It is noted that this study specifically

measured the effective turning radius, defined as the minimum radius suitable for a vehicle turning from a right-hand travel lane on the approach street to the appropriate lane of the receiving street (see Figure 18), rather than the curvature of the curb at the corner.

Figure 18. Effective turning radius
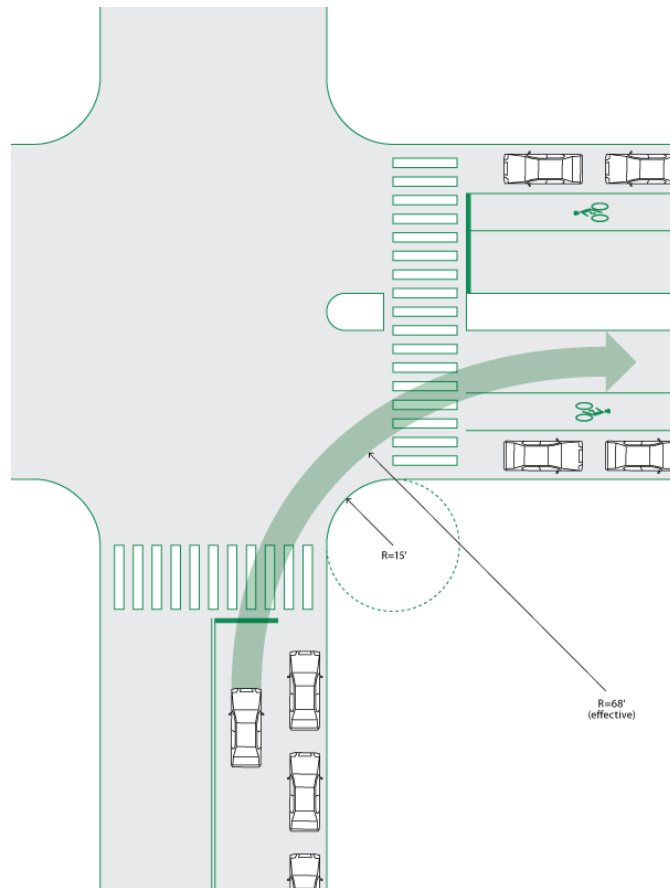
Fugro Roadware iVision5 is a web-based platform for data visualization and analysis, providing access to data collected by an Automated Road Analyzer (ARAN) and processed through the Vision software suite. Accessible through a web browser, iVision5 provides synchronized views of video logs, pavement images, and pavement condition data from any location. The platform records key roadway geometric attributes such as the number of lanes, lane width, approach grade, and area type. The user-friendly interface of iVision5 allows for detailed analysis of roadway features. In this study, iVision5 was used to extract the number of lanes, lane width, approach grade, and area type, ensuring accurate and consistent data collection for analysis. Figure 19 illustrates the iVision5 interface using available data.

Figure 19. Fugro iVision5 interface at a signalized intersection
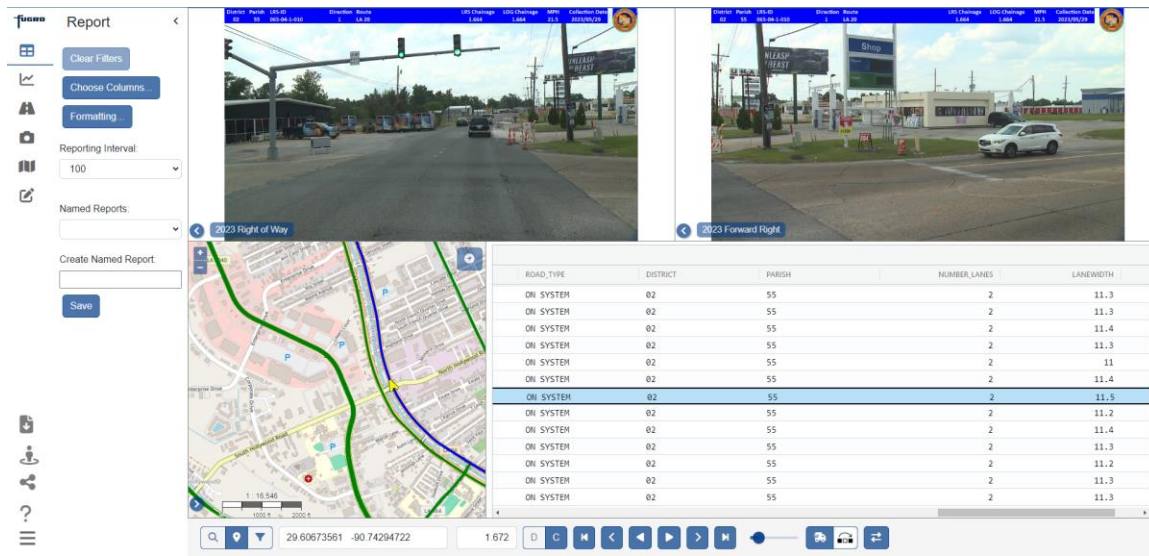
Regional Integrated Transportation Information System (RITIS) is a comprehensive platform designed for transportation analysis, monitoring, and data visualization. RITIS integrates data from various roadway sensors, including inductive loops, side-fired sensors (e.g., acoustic and microwave), radar, and video detection systems. It also incorporates probe-based data from agency-owned Bluetooth sensors and third-party providers such as HERE Technologies, INRIX, and TomTom. RITIS collects traffic volume data from the Highway Performance Monitoring System (HPMS) and provides detailed traffic volume information at the Traffic Message Channel (TMC) segment level. This platform provides traffic volume data for all roadway types, including local and rural roads, which is particularly beneficial for analyzing stop-controlled intersections located on local roads and in rural areas. Traditional platforms, such as MS2, often lack traffic volume data for these regions, posing challenges in obtaining accurate information. RITIS, however, offers reliable and precise traffic volume data for such locations, making it a suitable resource for this study. The interface is illustrated in Figure 20.

Figure 20. RITIS platform interface
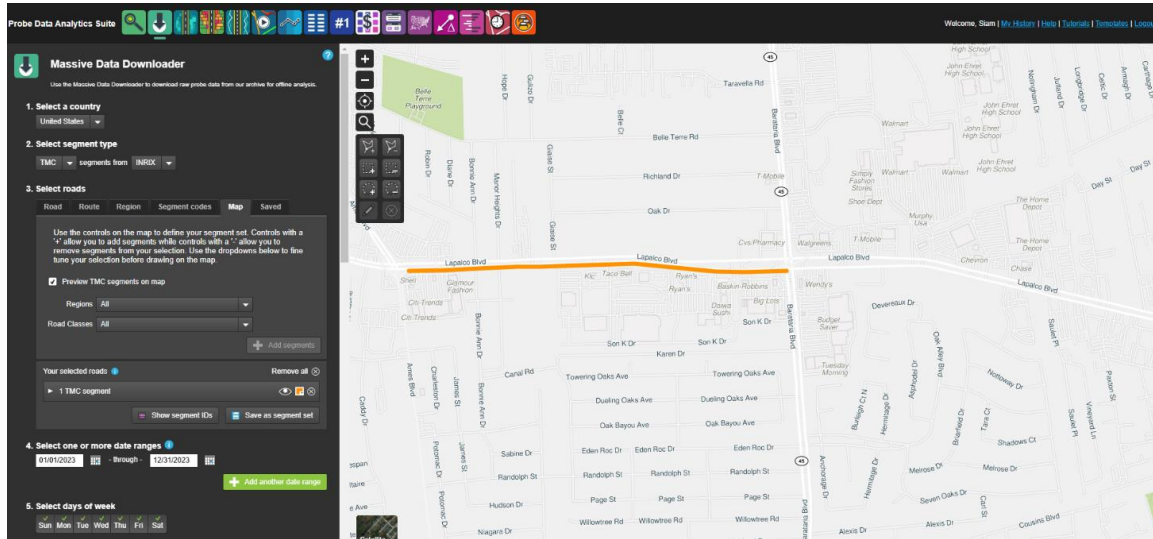
MS2 Traffic Count Database System is a cloud-based platform designed to manage and organize traffic count data for Louisiana and other states. It supports traffic analysis, volume forecasting, and reporting to the Federal Highway Administration (FHWA), facilitating data-driven transportation planning and decision-making. In this study, the MS2 platform was used to gather AADT data for locations not covered by the RITIS platform. Figure 21 shows an interface of MS2 with available traffic count locations.

Figure 21. MS2 Traffic Count interface
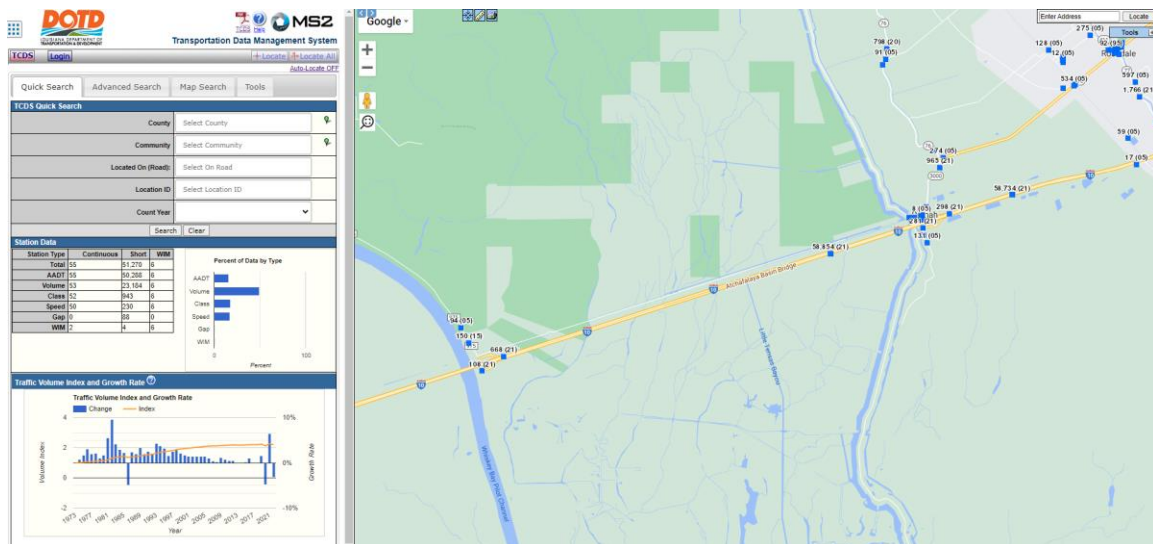
Data Description

A comprehensive database was developed from the collected data for both signalized and stop-controlled intersections to facilitate the analysis of factors influencing intersection capacity parameters. The influencing factors were identified based on a thorough review of relevant literature, their context-specific significance, and the availability of data. Since this study examines intersection capacity parameters for both signalized intersections and stop-controlled intersections, the subsequent sections are organized accordingly, with each section providing a detailed description of the data specific to the respective intersection type.

SFR Database

This study selected 24 variables to identify factors affecting SFR, considering attributes such as intersection and lane geometry, vehicle composition, and vehicle movements, among others. The final dataset consists of 1,080 rows, with each row representing a single cycle from an intersection. Table 8 provides descriptions of the variables used in the analysis, along with their mean values and standard deviations. The variables include temporal attributes (e.g., morning, mid-day, and evening peak hours), traffic characteristics (e.g., percentage of heavy vehicles and turning movements), geometric features (e.g., number of lanes, lane width, and turn radii), environmental factors (e.g., weather and pavement conditions), and contextual factors (e.g., area type, population, and access points near the intersection).

Table 8. Variable description and summary statistics of SFR analysis

Factors	Description of Factors	Mean	Standard Deviation
Morning_peak	Time of the day is morning peak hour (7:00 A.M. – 9:00 A.M.)	0.13	0.34
Mid_day	Time of the day is between morning and evening peak hours (9:00 A.M. – 3:00 P.M.)	0.56	0.50
Evening_peak	Time of the day is evening peak hour (3:00 P.M. – 6:00 P.M.)	0.23	0.42
% HV	Percentage of heavy vehicles present in the traffic during SFR estimation	4.91	11.31
% RLT	Percentage of right- or left-turning vehicles during saturation headway estimation	4.64	16.44
# Int Legs	Number of legs at the studied intersection	4.19	0.69
# of Lanes	Number of lanes at the studied approach	3.60	1.06
Exclusive Lane	The study approach is an exclusive through/left/right lane	0.56	0.49
Shared Lane	The study approach is a shared through-right/through-left lane	0.44	0.49
Ln_width	Lane width at the studied approach (in ft.)	11.12	0.57
App_grade	Grade of the studied approach	-0.01	0.49
Urban	Area type: Urban	0.96	0.20
Acc_point_yes	Yes if there is an access point within 250 ft. of the intersection	0.75	0.43
Speed_limit	Speed limit at the studied approach (in mph)	44.50	8.68
AADT	Average annual daily traffic (in thousands) at the studied approach	13.20	6.51
Int_gap	Gap between the studied intersection and the upstream intersection (in ft.)	1699.91	1441.28
R_turn_radi	Effective right-turn radius at the studied approach (in ft.)	50.10	18.47
L_turn_radi	Effective left-turn radius at the studied approach (in ft.)	69.99	35.46
Weather_clr	Weather condition: Clear	0.96	0.21
Pav_con_dry	Pavement condition: Dry	0.97	0.17
Ped_cross_yes	Yes if there is a pedestrian crossing at the studied intersection	0.12	0.33
Area_pop	Area population (in thousands) based on the ZIP code of the studied intersection	30.46	13.98

CH Database

A total of six variables were considered for factor analysis of CH, including movement type, intersection geometry, and traffic characteristics. The final dataset consists of 515 observations for left-turn movements, 397 observations for right-turn movements, and 302 observations for through movements. Table 9 provides a description of each variable considered, along with its mean and standard deviation.

Table 9. Variable description and summary statistics of CH analysis

Factors	Description of Factors	Mean	Standard Deviation
mvnt_type	Movement type of the subject vehicle (Left-turning = 1, Right-turning = 2, Through = 3)	1.82	0.80
hv	Indicator for heavy vehicles (1 = Heavy vehicle such as a bus or truck, 0 = Otherwise)	0.14	0.34
Num_rej_gap	Total number of gaps rejected by the subject vehicle	2.98	3.39
ln_cross	Total number of lanes the subject vehicle must cross to complete its movement	2.60	0.86
maj_sl	Speed limit of the major street (mph)	46.83	9.72
aadt_maj	Annual Average Daily Traffic (AADT) volume on the major street (in thousands)	8.11	5.57

Data Reduction

From the raw data, SFR for each cycle was computed and then aggregated using both unweighted and weighted averages, with the latter based on the number of vehicles. As each cycle in this study includes three observations of SFR, a coefficient of variation (CV) check was performed. The CV, a standardized measure of relative variability, is calculated as the ratio of the standard deviation to the mean, expressed as a percentage. It provides a means to compare variability across datasets with different scales. A higher CV indicates greater relative variability, while a lower CV reflects less relative variability. Typically, a CV less than 1 (or 100%) suggests low variance, whereas a CV exceeding 1 indicates high variance. In this study, for cycles where the CV of the observations exceeded 1, the observation with the highest variance was excluded. The average of the remaining observations was then considered as the SFR for that particular cycle. Figure 22 shows an image of the completed SFR workout sheet.

**Figure 22. Sample complete workout sheet for prevailing SFR estimation**

Counts	Elapsed Time (sec) 1	Total # Vehicles 1	Elapsed Time (sec) 2	Total # Vehicles 2	Elapsed Time (sec) 3	Total # Vehicles 3	# of Heavy Vehicles	# of R/L Turns	Calc SFR1	Calc SFR2	Calc SFR3	CV A	CV 1-2	CV 1-3	CV 2-3	Average SFR
1	11.57	4	12.03	4	12.11	4	0	0	1244.60	1197.01	1189.10	2.025	1.949	2.280	0.331	1193
2	7.03	3	7.1	3	7.05	3	0	1	1536.27	1521.13	1531.91	0.416	0.495	0.142	0.353	1530
3	7.79	3	7.86	3	7.82	3	0	1	1386.39	1374.05	1381.07	0.366	0.447	0.192	0.255	1381
4	11.06	4	11.23	4	11.09	4	0	1	1301.99	1282.28	1298.47	0.663	0.763	0.135	0.627	1294
5	8.73	3	8.88	3	8.76	3	0	1	1237.11	1216.22	1232.88	0.734	0.852	0.172	0.680	1229
6	11.96	4	11.98	4	12	4	1	1	1204.01	1202.00	1200.00	0.136	0.084	0.167	0.083	1202
7	12.06	4	11.89	4	12.01	4	1	3	1194.03	1211.10	1199.00	0.597	0.710	0.208	0.502	1201
8	14.54	6	14.68	6	14.59	6	0	0	1485.56	1471.39	1480.47	0.396	0.479	0.172	0.307	1479
9	21.36	11	21.11	11	20.99	11	0	0	1853.93	1875.89	1886.61	0.727	0.589	0.874	0.285	1872
10	17.09	9	17.17	9	17.33	9	0	0	1895.85	1887.01	1869.59	0.579	0.234	0.697	0.464	1884
11	19.52	8	19.44	8	19.32	8	0	0	1475.41	1481.48	1490.68	0.424	0.205	0.515	0.310	1483
12	20.51	9	20.36	9	20.41	9	0	0	1579.72	1591.36	1587.46	0.305	0.367	0.244	0.123	1586
13	21.12	11	22.1	11	21.55	11	0	0	1875.00	1791.86	1837.59	1.853	2.267	0.985	1.260	1792
14	9.41	5	9.33	5	9.4	5	0	0	1912.86	1929.26	1914.89	0.380	0.427	0.053	0.374	1919
15	16.85	8	16.96	8	16.99	8	0	0	1709.20	1698.11	1695.11	0.356	0.325	0.414	0.088	1701
16	19.67	9	19.54	9	19.69	9	0	0	1647.18	1658.14	1645.51	0.339	0.332	0.051	0.382	1650
17	14.13	6	14.27	6	14.21	6	1	0	1528.66	1513.67	1520.06	0.404	0.493	0.282	0.211	1521
18	10.17	3	10.22	3	10.05	3	0	0	1061.95	1056.75	1074.63	0.705	0.245	0.593	0.839	1064
19	21.17	9	22.09	9	21.47	9	0	0	1530.47	1466.73	1509.08	1.763	2.127	0.704	1.423	1520
20	13.63	6	13.45	6	13.39	6	0	0	1584.74	1605.95	1613.14	0.753	0.665	0.888	0.224	1601

	Average	1505
	Weighted Average	1583
	Median	1520

To ensure data accurately reflected typical local driver behavior, cycles with unusually large lost time due to driver distraction were excluded from the analysis. Figures 23 and 24 illustrate an example of exceptionally high lost time caused by driver distraction and provide a thematic visualization of total lost time components. These atypical observations were deliberately removed to prevent extreme bias in the results.

Figure 23. Possible distracted driver in the queue

Figure 24. Thematic visualization of effect of total lost time due to distraction
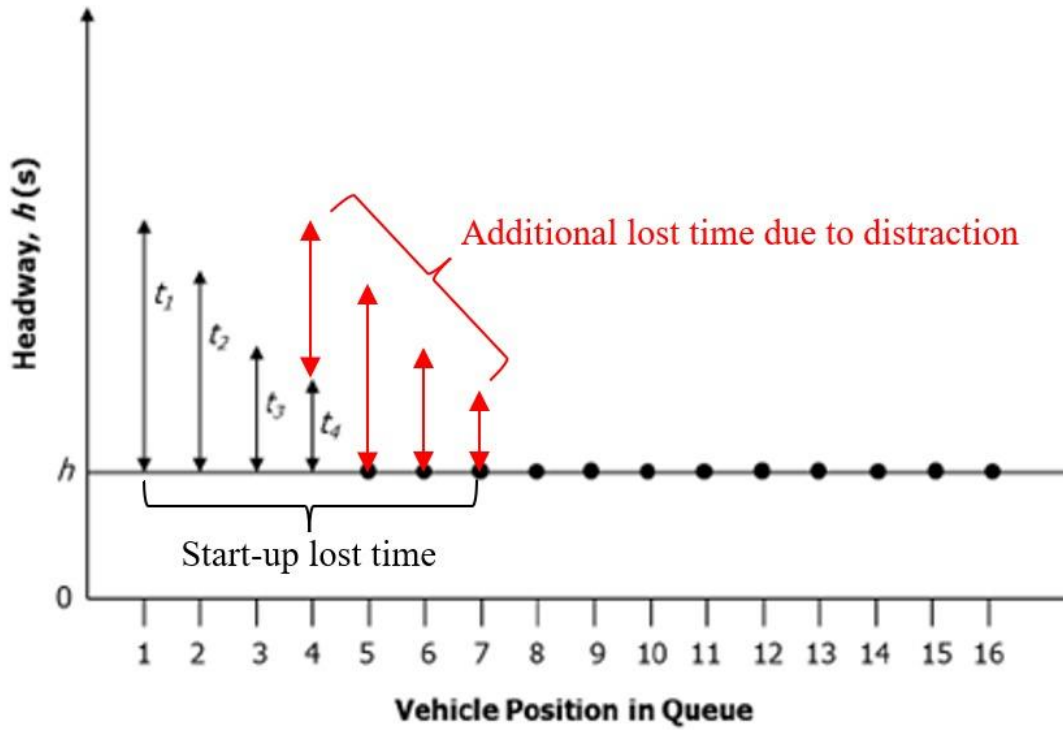
For each intersection, both rejected and accepted gaps were observed for CH. A minimum of 25 data points was considered for each intersection. In cases where a vehicle accepted a gap without rejecting any, the maximum rejected gap was recorded as 0.1 sec. If an excessive number of vehicles accepted a gap without rejecting any, those vehicles were excluded from the analysis database, provided that sufficient data were available from vehicles that had both rejected and accepted gaps. Additionally, at intersections with low major road traffic volume, there were instances where the accepted gap exceeded 60 sec. These observations were also excluded from the database.

A similar approach was applied to FH data. Instances where the following vehicle took an excessively long time (more than 20 sec.) were removed from the analysis database. Visibly distracted drivers who failed to utilize potentially acceptable gaps were also excluded based on the observer's judgment to avoid bias in the estimation of CH and FH.

Discussion of Results

This chapter presents and discusses the analysis results from this study. The findings are organized into two primary sections: the first focuses on the estimation of SFR and the factors influencing it, while the second addresses the estimated CH and FH, exploring the factors affecting these parameters. The chapter concludes with recommendations for intersection capacity parameter values specific to Louisiana.

Analysis Results for SFR

The estimated base SFR values for each signalized intersection were analyzed to determine the average base SFR for the state, including the off-peak hours. Table 10 presents the results of the statistical analysis of saturation flow rates across all intersections, while Figure 25 illustrates the distribution of SFR values at the signalized intersections included in the study.

Table 10. Summary statistics of base SFR

	Saturation Flow Rate
Mean	1655
Median	1646
Standard Deviation	127

Figure 25. SFR distribution across the signalized intersections of Louisiana
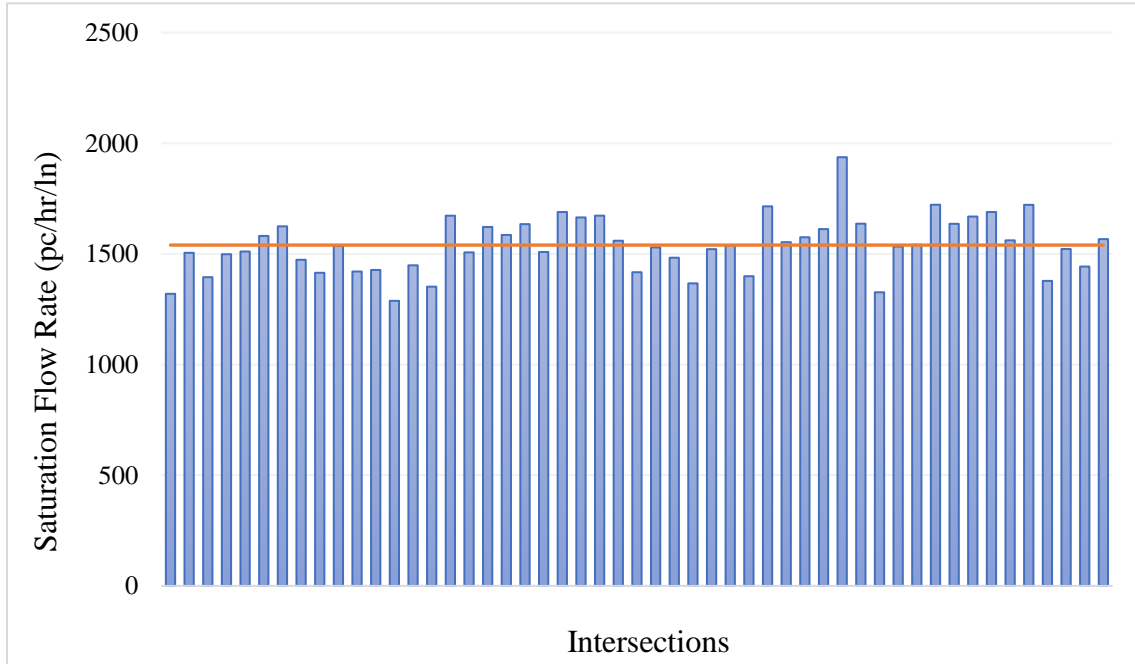
The mean base SFR for Louisiana was estimated to be 1,655 passenger cars per hour of green per lane. The standard deviation of 127 pc/hr/ln indicates a moderate level of variability in SFR across the studied intersections, reflecting differences in intersection characteristics, geometric configurations, or prevailing traffic flow conditions.

Factors Affecting SFR From Cycle Data

The feature selection process utilized univariate analysis to evaluate the relationship between each predictor and the dependent variable. This approach identified variables with strong statistical associations to the target outcome, retaining only those with significant predictive power for the modeling phase and eliminating redundant or non-informative predictors [78] [79]. Univariate analysis assesses each predictor individually, prioritizing those with the greatest potential to enhance model performance, thereby streamlining the feature set for predictive modeling.

Table 11 presents the results of the univariate analysis conducted on the variables considered in this study. Predictor significance was assessed using p-values, with variables exhibiting a p-value greater than 0.05 excluded from the prediction models. Of the 25 variables initially evaluated, 16 demonstrated a statistically significant relationship with the dependent variable and were subsequently included in the modeling process.

Table 11. Feature selection

Variables	Estimate (P-Value)
Mid-day (9:00 A.M. - 2:59 P.M.)	-47.77 (0.0046)
Evening peak (3:00 P.M. - 6:00 P.M.)	61.68 (0.0018)
Percentage of heavy vehicles	-8.53 (<0.0001)
Percentage of turning movement (right/left)	-2.73 (<0.0001)
Number of intersection leg	34.02 (0.0048)
Number of lanes	54.46 (<0.0001)
Exclusive lane	106.99 (<0.001)
Shared lane	-106.99 (<0.001)
Lane width	41.31 (0.0051)
Approach grade	37.76 (0.0259)
Speed limit	4.43 (<0.0001)
Intersection gap	0.03 (<0.0001)
Area population	1.64 (0.0063)

Later, LASSO regression was employed to identify the key factors influencing SFR. This modeling approach selected a combination of geometric, traffic, and operational characteristics of signalized intersections that significantly impact SFR. The selected variables exhibited both positive and negative associations with SFR, indicating the varying nature of their influence. Figure 26 illustrates the key factors affecting prevailing SFR at signalized intersections.

Figure 26. Factors affecting cycle level prevailing SFR
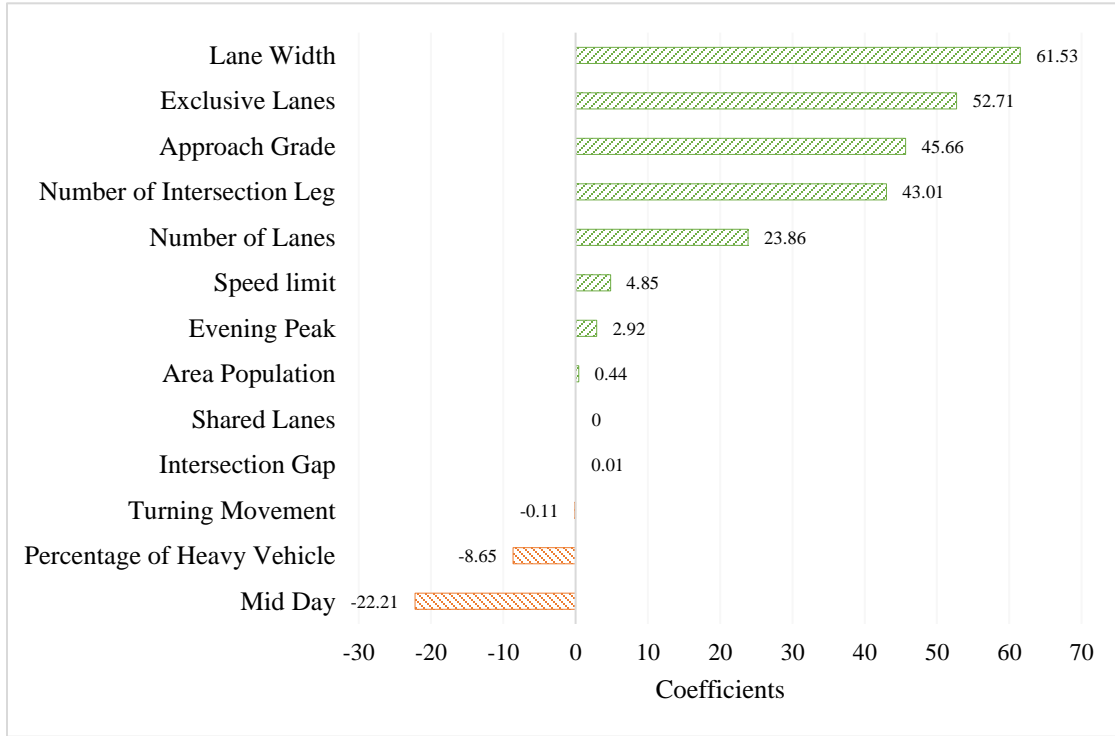
Among the positive contributors to prevailing SFR at cycle level, lane width (61.53) emerged as the most influential factor, indicating that wider lanes enhance SFR at signalized intersections [31]. Vehicles traveling through narrower lanes tend to maintain greater spacing, resulting in longer gaps and reduced flow rates [80]. Additionally, wider lanes reduce side friction, thereby improving traffic movement efficiency and increasing SFR [81].

The presence of exclusive lanes (52.71) also showed a strong positive association with SFR, as exclusive lanes reduce lane-changing conflicts and delays caused by slower turning vehicles, improving overall lane utilization. Approach grade (45.66) demonstrated a positive influence on SFR as well. This may be attributed to the fact that negative grades can introduce speed variations, increased braking, and longer reaction times, which negatively impact flow, whereas moderate positive grades may not substantially hinder vehicle progression.

The number of intersection legs (43.01) was also positively associated with SFR. Signalized intersections with more legs often include dedicated and wider lanes, along with optimized signal phasing, which collectively enhance traffic flow. Further, an increase in the number of lanes (23.86) was positively correlated with SFR, as more lanes allow for higher vehicular throughput and facilitate smoother merging and maneuvering within the intersection,

resulting in shorter headways and reduced clearance times [9] [28] [29] [82]. Additional factors such as speed limit (4.85), evening peak hours (2.92), and area population (0.44) also exhibited minor positive effects on SFR.

On the other hand, several variables were identified as negative contributors to SFR. SFR was found to decrease during mid-day hours (-22.21), likely due to lower traffic volumes compared to peak periods, which may result in less efficient utilization of green time. The percentage of heavy vehicles (-8.65) also had a notable negative effect on SFR. Heavy vehicles typically accelerate more slowly, occupy more space, and disrupt flow continuity, thereby lowering overall SFR [9] [82] [83]. Their presence can also influence passenger car behavior, prompting increased headways, deceleration, and lane changes, further degrading flow efficiency [84].

The percentage of turning vehicles (-0.11), though a smaller contributor, also negatively affected SFR. Turning movements generally require longer maneuver times, create additional conflict points, and reduce the effective capacity for through traffic [40]. Lastly, the shared lane variable had a near-zero coefficient (0.000), suggesting that after controlling for other factors, the presence of shared lanes did not have a substantial independent impact on SFR within the dataset analyzed.

The LASSO regression equation for SFR estimation is:

$$
\begin{aligned}
SFR = {}& 373.9965 + (61.5308 * Lane\,Width) + (52.7128 * \\
& Exclusive\,Lane) + (45.6570 * Approach\,Grade) + (43.0103 * \\
& Number\,of\,Intersection\,Leg) + (23.8659 * Number\,of\,Lane) + (4.8530 * \\
& Speed\,Limit) + (2.9193 * Evening\,Peak) + (0.4366 * Area\,Population) + \\
& (0.0105 * Intersection\,Gap) - (1.1044 * \%\,of\,Turning\,Movement) - \\
& (8.6472 * \%\,of\,Heavy\,Vehicle) - (22.2116 * Mid\,Day) \qquad (13)
\end{aligned}
$$

Base SFR for Louisiana by Districts

The base saturation flow rate (BSFR) was calculated for 51 signalized intersections across Louisiana, accounting for observed variations in lane width (average 11.2 ft.), heavy vehicle presence (average 4.4%), right-turn movements (average 6.6%), and left-turn movements (average 1.4%). After applying these adjustments, the statewide BSFR was determined to be 1,655 pc/h/ln, which is 13% lower than the HCM default of 1,900 pc/h/ln, reflecting the influence of local traffic conditions on intersection capacity. As Figure 27 illustrates, the highest BSFR was observed in District 61 (Baton Rouge) at 1,773 pc/h/ln, while the lowest

was in District 3 (Lafayette) at 1,537 pc/h/ln, reflecting the range of local traffic conditions across the state.

Figure 27. Base SFR by district and statewide
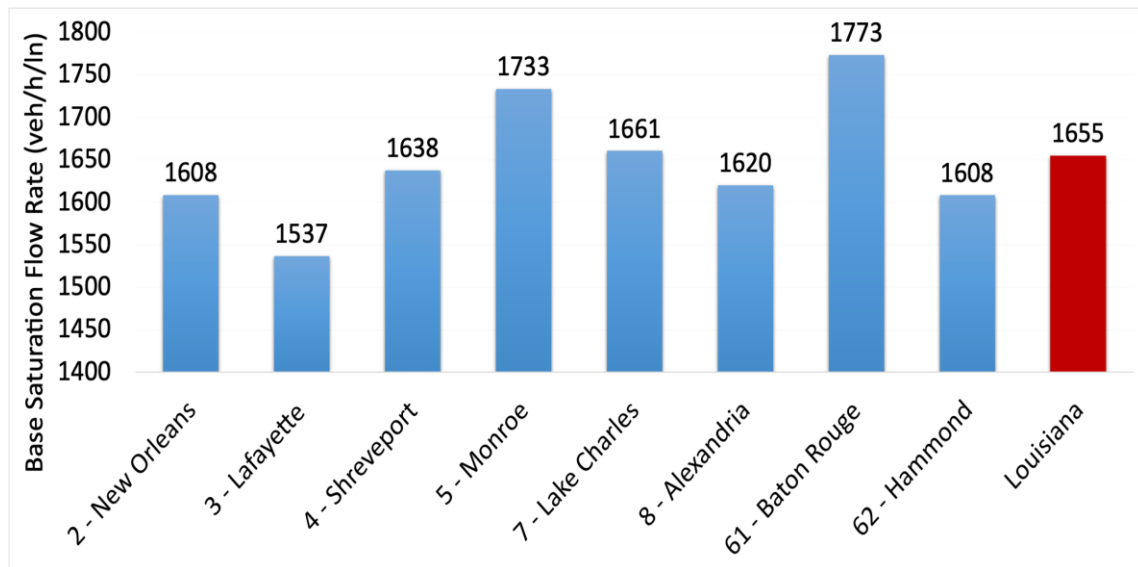
Comparison with Other Jurisdictions in U.S.

Figure 28 illustrates significant regional variation in SFR across different states. Louisiana's measured average SFR (blue bar) is 1,582 vehicles per hour per lane, placing it below Maryland (2,080), Florida (1,950), and Pennsylvania (1,800). Similarly, Louisiana's Base SFR (orange bar) of 1,655 vehicles per hour per lane is 12.89% lower than the HCM standard of 1,900 vehicles per hour per lane, while also falling below Indiana's Base SFR range (1,352-2,178) and New Jersey's range (1,900-2,100).

Figure 28. Comparison of estimated Louisiana SFR with other states
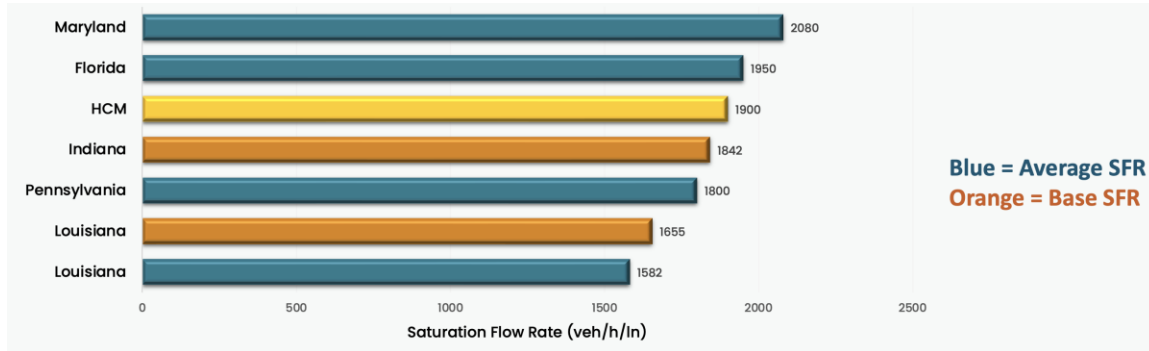
Variation of SFR with Highway Functional Class and AADT

In order to explore the impact of exposure on Base SFR values, which were derived from prevailing SFR measurements, an analysis was conducted to determine how these values may be influenced by traffic pressure resulting from AADT and highway functional classification. The results of classification by highway functional class (Figure 29) show that Principal Arterials have a higher BSFR (1,684 pc/h/ln) compared to Minor Arterial and Collector roadways (1,579 pc/h/ln). A classification by AADT (Figure 30) reveals a clear relationship between traffic volume and BSFR. Locations with AADT ≥ 18,752 exhibited the highest BSFR (1,743 pc/h/ln), while medium-volume locations (5,818 ≤ AADT < 18,752) showed a BSFR of 1,654 pc/h/ln, and low-volume locations (AADT < 5,818) had the lowest BSFR (1,575 pc/h/ln). In Figures 29 and 30, the *n* value indicates the number of intersections fall in the group.

Figure 29. Base saturation flow rate results by highway functional class
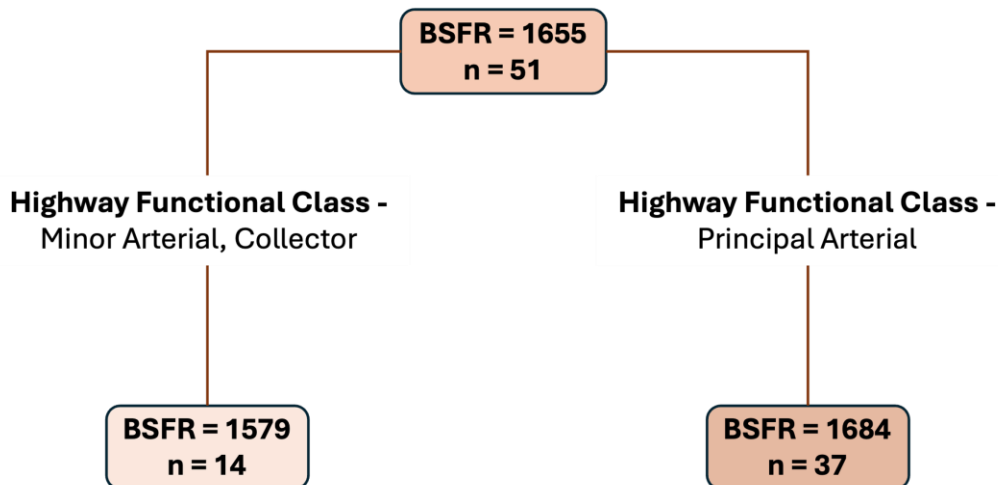
Figure 30. Base saturation flow rate results by AADT
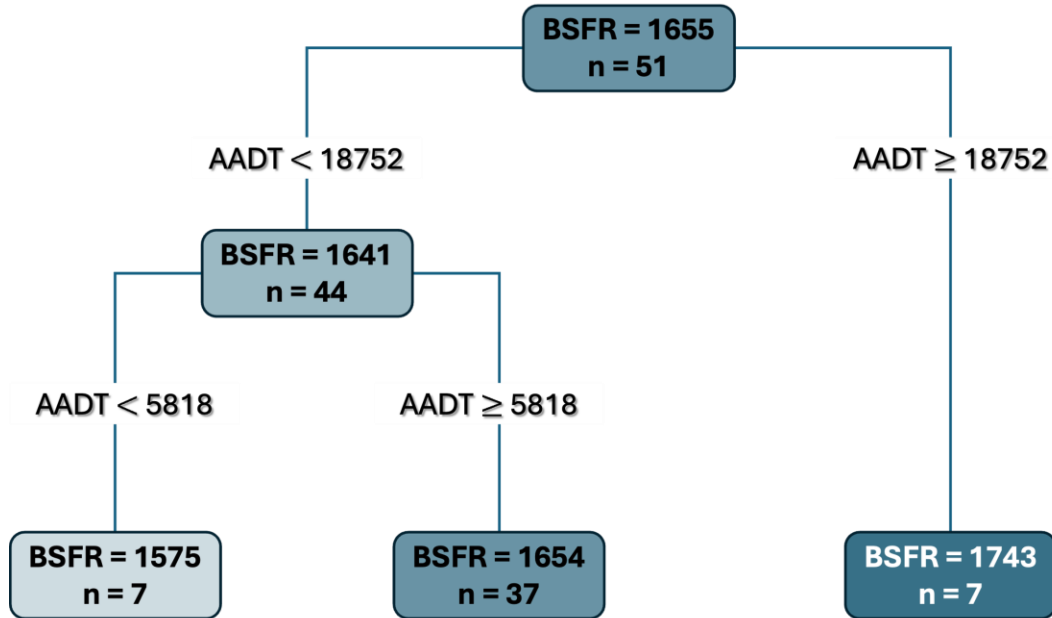
Analysis Results for CH Estimation

In this study, as presented in Table 12, the mean critical headway (CH) was estimated considering two intersection types: Type 1, consisting of a single-lane minor street and single-lane major street in each direction, and Type 2, consisting of a single-lane minor street and multi-lane major street in each direction. Additionally, CH was evaluated for three types of minor street movements: left-turn, right-turn, and through movements. This classification was primarily based on the number of lanes a vehicle must cross, which reflects the complexity and difficulty of the maneuver. For example, at Type 1 intersections, a left-turning vehicle from the minor street must cross two lanes, one in each direction, requiring the driver to identify an acceptable gap in both lanes of opposing traffic on the major street. In contrast, at Type 2 intersections, where the major street includes multiple lanes in each direction, the driver must assess gaps across several lanes in the same direction, further increasing the complexity of the maneuver.

For right-turning movements, the driver typically needs to evaluate only one conflicting lane, regardless of whether the intersection is Type 1 or Type 2. Table 13 presents the estimated mean CH values categorized by intersection type and minor street movement, providing insights into how intersection layout and movement type influence gap acceptance behavior.

Table 12. Geometric configurations of TWSC intersection
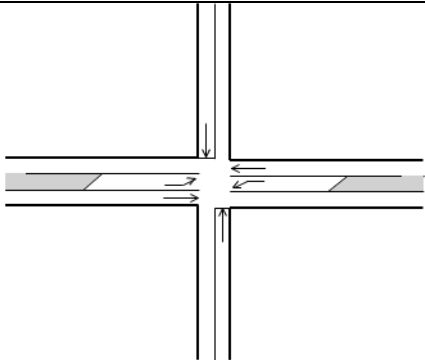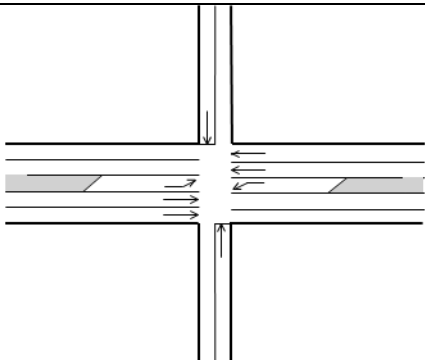
Type 1 TWSC intersection

Lanes on major street = 1
Lanes on minor street = 1
Major street exclusive left-turn lane (optional)

Type 2 TWSC intersection

Lanes on major street = 2 or more
Lanes on minor street = 1
Major street exclusive left-turn lane (optional)

Table 13. Estimated values of CH for Louisiana

Geometry	Type 1 Single Lane Major Street			Type 2 Multi-lane Major Street		
Movement	MinLT	MinRT	MinTH	MinLT	MinRT	MinTH
Mean Critical Headway (sec)	9.9	8.7	8.9	10.1	7.1	9.7
Standard Deviation	1.6	2.2	1.9	1.6	0.7	1.4

The results indicate that the CH is higher for left-turn and through movements of minor street vehicles at Type 2 stop-controlled intersections compared to Type 1 intersections. This outcome is expected, as vehicles at Type 2 intersections must cross a greater number of lanes, resulting in an increased number of conflict points. Interestingly, the CH for right-turn movements from the minor street is 1.6 sec. lower at Type 2 intersections than at Type 1. Regardless of intersection type, right-turning vehicles encounter only one conflict point with major street traffic traveling in the rightmost lane. At Type 2 intersections, where multiple lanes are present in each direction, major street vehicles are more likely to occupy the left lanes, thereby reducing conflicts in the rightmost lane and allowing minor street right-turning vehicles to accept shorter gaps.

Factors Affecting Critical Headway

LASSO regression was applied to identify the factors influencing CH at TWSC intersections in Louisiana and to develop corresponding predictive equations. To ensure the model accurately captured the key influencing factors across various traffic scenarios, separate regression models were developed for each movement type. Additionally, a combined model was formulated to incorporate all movement types. Table 14 presents the identified factors influencing CH for each movement category, while Equations 14-17 provide the regression equations for the individual movement types, as well as the combined model.

Table 14. Factors affecting critical headway

Movement	Variables	Coefficients
Minor street left turn	Number of heavy vehicles	0.0593
	Major street AADT	-0.1905
Minor street right turn	Number of heavy vehicles	0.6885
	Major street speed limit	0.0967
	Major street AADT	-0.0762
	Number of rejected gap	-0.0772
	Number of lanes on major street	-0.2324
Minor street through	Number of heavy vehicles	0.6009
	Major street speed limit	0.0617
	Number of rejected gap	0.0295

Minor Street Left Turn (R2 = 0.41):

$$CH_{MinorLt} = 11.0158 + (0.0593 * heavy\_vehicle) - (0.1905 * aadt\_maj) \quad (14)$$

Minor Street Right Turn (R2: 0.49):

$$CH_{MinorRt} = 5.2334 + (0.6885 * h\_veh) + (0.0967 * maj\_sl) - (0.0762 * aadt\_maj) - (0.0776 * num\_rej\_gap) - (0.2324 * num\_maj\_ln) \quad (15)$$

Minor Street Through (R2 = 0.26):

$$CH_{MinorTh} = 6.2995 + (0.6009 * h\_veh) + (0.0617 * maj\_sl) + (0.0295 * num\_rej\_gap) \quad (16)$$

Combined (R2 = 0.46):

$$CH = 6.7309 + (0.3564 * h_{veh}) + (0.2559 * cross) + (0.0607 * maj_{sl}) - (0.0633 * num_{maj_{ln}}) - (0.1152 * aadt\_maj) \tag{17}$$

The regression analysis results indicate that CH for minor street left-turn movements increases when the subject vehicle is a heavy vehicle. This finding aligns with expectations, as heavy vehicles typically have slower acceleration rates, requiring more time to merge into major street traffic and thus necessitating larger gaps compared to passenger cars [71] [74]. Conversely, major street AADT was found to negatively influence CH, indicating that as traffic volume increases, the availability of acceptable gaps decreases, often compelling drivers to accept smaller gaps [72] [85].

For right-turn movements, vehicle type and major street traffic volume similarly affect CH. Additionally, other factors were found to be significant. CH increases with higher major street speed limits, as faster-moving vehicles reduce drivers' reaction time and increase uncertainty in judging safe gaps, thereby prolonging waiting times [86] [87]. Conversely, CH decreases as the number of rejected gaps increases, suggesting that after multiple unsuccessful attempts, drivers become more inclined to accept shorter gaps, potentially compromising safety [72] [73]. Further, the number of lanes on the major street was found to negatively influence CH for right-turning movements. Right-turning drivers typically seek a gap in the rightmost lane; with more lanes, traffic tends to be distributed across multiple lanes, reducing flow intensity in any single lane and increasing the frequency of acceptable gaps, thereby lowering CH.

For through movements, CH was influenced by vehicle type, major street speed limit, and the number of rejected gaps, all of which were associated with increased CH, reflecting greater hesitation or difficulty in accepting suitable gaps under these conditions.

Analysis Result for FH Estimation

For FH estimation, the mean value was determined based on the movement type of the following vehicle. Table 15 presents the mean values of FH across different movement types. Clearly, through movement had higher FH estimates than those of turning movements.

Table 15. Estimated follow-up headway values for Louisiana

Movement	MinLT	MinRT	MinTH
Mean Follow-up headway (FH)	5.9	5.8	6.5
Standard Deviation	1.7	2.4	1.3

Table 16 shows a comparison between the range of estimated values for Louisiana and the default values range provided in the Highway Capacity Manual (HCM). The values estimated in Louisiana are significantly higher than the default values of the HCM. The estimated Louisiana values are indicative of Louisiana traffic conditions on TWSC minor roads, reflecting driving behavior as well.

Table 16. Comparison of default CH and FH values with Louisiana values

Parameters	Default HCM values	Estimated values for Louisiana
Critical Headway, CH (sec.)	4.1 - 7.3	7.1 – 10.1
Follow-up Headway, FH (sec.)	2.2 – 4	5.9 – 6.5

Conclusions

Intersection capacity parameters (SFR, CH, and FH) play an important role in accurate capacity estimation and signal design, ultimately impacting network-level transportation planning. Therefore, accurately estimating these parameters is essential. While the HCM provides default values for intersection capacity parameters, HCM states that these values may vary based on geographic location due to unique geographic characteristics, local traffic conditions, and other influential factors. Efficient capacity estimation allows planners to design and manage intersections by predicting congestion, optimizing signal timings, and deciding on infrastructure improvements.

This study estimated and recommended intersection capacity parameter values specific to Louisiana. Additionally, it identified the factors affecting SFR and CH and developed predictive models for both parameters. A comprehensive literature review examined methodologies for estimating intersection capacity parameters (SFR, CH, FH) across various jurisdictions, analyzing peer-reviewed journals and government reports with an emphasis on empirical field studies rather than theoretical approaches. The review is organized by intersection type: signalized intersections (SFR) and stop-controlled intersections (CH and FH), providing the foundation for developing locally estimated parameters for Louisiana's signalized and TWSC intersections.

After a selection approach from 511 systems, highway section data, and DOTD district representatives, a total of 77 intersections (51 signalized and 26 TWSC intersections) across eight districts in Louisiana were analyzed. Traffic data were collected using video recordings, and supplementary data, including intersection geometry, geographic characteristics, and traffic conditions.

A collective analysis of compiled data from selected signalized intersections was conducted using a regression approach to identify key factors influencing cycle-by-cycle SFR. Regression analysis identified several factors influencing SFR: intersection geometry (e.g., lane width, presence of exclusive lanes, approach grade, and number of intersection legs), speed limit, and traffic hour positively influenced SFR by increasing its value, while the presence of heavy vehicles and off-peak hours had a negative impact.

Using the adjustment approach outlined in the HCM, the base-adjusted SFR for signalized intersections in Louisiana was estimated at 1,655 pc/hr/ln. Compared to the HCM default recommended value of 1,900 pc/hr/ln, this finding suggests that the average SFR at

signalized intersections in Louisiana is significantly lower than the HCM default value. The highest BSFR was observed in District 61 (Baton Rouge) at 1,773 pc/h/ln, while the lowest was in District 3 (Lafayette) at 1,537 pc/h/ln, reflecting the range of local traffic conditions across the state.

This study derived local critical headway (CH) and follow-up headway (FH) values for two-way stop-controlled (TWSC) intersections to enhance capacity analysis accuracy in Louisiana. CH values, calculated using Maximum Likelihood Estimation (MLE), ranged from 7.1 to 10.1 sec., significantly higher than the HCM range of 4.1 to 7.3 sec. These values increased with heavy vehicles, number of rejected gaps, and major street speed limits, while decreasing with major street AADT and number of lanes. Similarly, FH values determined through direct estimation ranged from 5.9 to 6.5 sec. depending on movement type, exceeding the HCM defaults of 2.2 to 4 sec. These higher values accurately reflect local driving behavior at Louisiana's predominantly low-volume TWSC intersections. Table 17 presents the HCM-recommended values for each intersection capacity parameter alongside the estimated values for Louisiana.

Table 17. Comparison of estimated parameters with HCM default values

Parameters	Default HCM values	Estimated values for Louisiana
Base Saturation Flow Rate, BSFR (pc/h/ln)	1,900	1,637
Critical Headway, CH (sec)	4.1 - 7.3	7.1 – 10.1
Follow-up Headway, FH (sec)	2.2 – 4	5.9 – 6.5

Recommendations

The fundamental recommendation for applying new intersection capacity parameters for signalized and TWSC intersections in Louisiana stems from the following HCM principle:

> *"Although the HCM provides default values for its methodologies, the analyst should be mindful that they represent typical national values and that typical conditions within a state, region, or community may be different. When default values are applied frequently in analyses, the use of local default values can help reduce the uncertainty in the analysis results."*

This study evaluated the locally adjusted base saturation flow rate (BSFR) across 51 signalized intersections in Louisiana, focusing on the influence of regional traffic dynamics on intersection performance. The BSFR represents the expected average flow rate for a through-traffic lane under exceptionally favorable geometric and traffic conditions (e.g., no grade, no trucks, etc). Louisiana's estimate is 1,655 pc/h/ln. In practice, the prevailing SFR should be estimated from this BSFR by adjusting for prevailing geometric and traffic conditions; Equation 1 (HCM 7th edition Eq 19-8) lists those adjustments that can be made for estimating prevailing SFR.

In the process of estimating prevailing SFR, adjustments can be made based on observed factors such as lane width, heavy vehicle presence, right-turn movements, and left-turn movements, as well as other applicable factors identified in Equation 1 (HCM 7th edition Eq 19-8). The statewide BSFR averaged 1,655 pc/h/ln, a 13% reduction from the HCM default of 1,900 pc/h/ln, indicating a reflection of local driving behavior and traffic patterns at signalized intersections that differ from HCM standards. The BSFR variation across districts is summarized below:

- District 2 (New Orleans): 1,608 pc/h/ln

- District 3 (Lafayette): 1,537 pc/h/ln

- District 4 (Shreveport): 1,638 pc/h/ln

- District 5 (Monroe): 1,733 pc/h/ln

- District 7 (Lake Charles): 1,661 pc/h/ln

- District 8 (Alexandria): 1,620 pc/h/ln

- District 61 (Baton Rouge): 1,773 pc/h/ln

- District 62 (Hammond): 1,608 pc/h/ln

The adjusted BSFR offers a district-wide estimate, facilitating a planning-level baseline for decisions across the entire district and supporting broader-scale planning efforts. However, caution is advised when applying it to infrastructure decisions for individual intersections. For signal improvements, infrastructure upgrades, or changes in intersection type, it is advisable to apply specific adjustments using the HCM manual tailored to each intersection to ensure accuracy and effectiveness. Based on the study's findings and associated correlation with traffic exposure and highway functions, the recommended values are outlined in Table 18 with specified criteria.

Table 18. Recommended values of Base SFR

Category	Application Criteria	Sub-Category	Base SFR (pc/h/ln)
Statewide	Broad scale planning level; instead of default HCM value of 1,900 pc/h/ln, adjustment will be required according to the factors in HCM 7th edition Eq 19-8 to estimate the prevailing SFR.	All Districts	1,655
District	If planning and operational analysis encompass a whole district, adjustment will be required according to the factors in HCM 7th edition Eq 19-8 to estimate the prevailing SFR.	District 2	1,608
		District 3	1,537
		District 4	1,638
		District 5	1,733
		District 7	1,661
		District 8	1,620
		District 58*	1,655
		District 61	1,773
		District 62	1,608
Highway Functional Class	If planning and operational analysis encompass multiple districts with the same functional class. Otherwise, the statewide Base SFR value of 1,655 pc/h/ln should take precedence. Adjustment will be required according to the factors in HCM 7th edition Eq 19-8 to estimate the prevailing SFR.	Principal Arterial	1,684
		Lower functional class	1,579
Average annual daily traffic (AADT)	If planning and operational analysis encompass multiple districts within the same AADT group. Otherwise, the statewide Base SFR value of 1,655 pc/h/ln should take precedence. Adjustment will be required according to the factors in HCM 7th edition Eq 19-8 to estimate the prevailing SFR.	AADT $\geq$ 18752	1,743
		18752 $>$ AADT $\geq$ 5818	1,654
		AADT $<$ 5818	1,575

Note: *The default state estimate value should be used here since no data has been collected for District 58.

In terms of TWSC operations, the higher values compared to HCM defaults remain relevant for TWSC intersections, as they are predominantly situated at low-volume minor roads, capturing realistic local conditions and an upgrade from HCM estimates. Planners are advised to still apply these values cautiously, CH (7.1 to 10.1 sec.) and FH (5.9 to 6.5 sec). For a relatively large number of intersections that need more precise applications, CH equations should be used reflecting the impact of heavy vehicles and other roadway factors.

Planners can further validate these parameters for specific intersection improvements when necessary—for example, when implementing physical measures to improve capacity or when establishing benchmark capacity estimates for future configuration improvements, such as conversion to signalized intersections and roundabouts.

When implementing these intersection capacity parameters (BSFR, CH, FH) in simulation or traffic analysis software, engineers are advised to take specific precautions. For large-scale applications, a thorough examination is needed for all interconnected attributes that will require adjustment as a result of changing the base parameters. For small-scale applications, further validation can be made for the estimated capacity parameters through field observations or historical data before implementation, ensuring all dependent variables are appropriately calibrated or adjusted, if needed, to maintain system consistency.

This study's scope was limited to four-leg signalized intersections and TWSC for consistency and to avoid bias. Due to visual limitations in camera placement, in several cases the estimations were made by averaging estimates for multiple lane groups. Additionally, future studies can be expanded to intersection types with different configurations to establish a broader baseline, or to different intersection types such as roundabouts. Although this study estimates the local parameters in a post-COVID, somewhat stable traffic condition, future planning at statewide and metropolitan levels may require further calibration with consideration of the project life cycle.

In the future, advanced technologies can be utilized, if available, to enhance real-time capacity estimates with greater precision. Louisiana's ongoing effort for Transportation Systems Management and Operations (TSMO) implementation could enable agencies to approach regional transportation as an interconnected network, optimizing traveler experience and system performance through improved multimodal management. Future updates of real-time intersection capacity estimates can strengthen these initiatives, particularly with V2X (vehicle-to-everything) deployment and coordinated adaptive intersection operations. Further, capacity adjustment factors should be developed for various penetration levels of connected and automated vehicles (CAVs) to adapt existing HCM methodologies for emerging CAV applications.

Acronyms, Abbreviations, and Symbols

Term	Description
AASHTO	American Association of State Highway and Transportation Officials
AADT	Annual Average Daily Traffic
ARAN	Automated Road Analyzer
BLM	Binary Logit Model
BSFR	Base Saturation Flow Rate
CBDs	Central Business Districts
CCTV	Closed Circuit Television
CDF	Cumulative Distribution Function
CH	Critical Headway
CV	Coefficient of Variation
DOTD	Department of Transportation and Development
FH	Follow-up Headway
FHWA	Federal Highway Administration
HCM	Highway Capacity Manual
HMM	Hidden Markov Model
HPMS	Highway Performance Monitoring System
hr	hour(s)
ln	lane(s)
LTRC	Louisiana Transportation Research Center
m	meter(s)
MLE	Maximum Likelihood Estimation
MLM	Modified Raff Method
OLS	Ordinary Least Squares
OTM	Occupancy Time Method
PCU	Passenger Car Units

Term	Description
PEM	Probability Equilibrium Method/Equation
RITIS	Regional Integrated Transportation System
SFR	Saturation Flow Rate
SUV	Sport Utility Vehicle
SVM	Support Vector Machines
TMC	Traffic Message Channel
TRRL	Transport and Road Research Laboratory
TSMO	Transportation Systems Management and Operations
TWSC	Two-Way Stop Controlled

References

[1]   R. B. Barnett-Woods, "How Roadway Capacity and Safety Intersect with Vision Zero Goals," [Online]. Available: https://ggwash.org/view/79050/how-roadway-capacity-and-safety-intersect-with-vision-zero. [Accessed 14 January 2025].

[2]   S. J. Rodke, S. D. Ghodmare and A. Deshmukh, "Critical Analysis of Saturation Flow Rate and Affecting Parameters," in *2022 10th International Conference on Emerging Trends in Engineering and Technology—Signal and Information Processing (ICETET-SIP-22)*, April 2022, pp. 1–6, doi: 10.1109/ICETET-SIP-2254415.2022.9791785.

[3]   N. Wu and S. Giuliani, "Capacity and Delay Estimation at Signalized Intersections Under Unsaturated Flow Condition Based on Cycle Overflow Probability," *Transp. Res. Procedia*, vol. 15, January 2016, pp. 63–74, doi: 10.1016/j.trpro.2016.06.006.

[4]   "Highway Capacity Manual—An Overview | ScienceDirect Topics," [Online]. Available: https://www.sciencedirect.com/topics/engineering/highway-capacity-manual. [Accessed 14 January 2025].

[5]   J. Codjoe, R. Thapa, S. M. A. Ayernor and M. Loker, "Determining Louisiana's Roundabout Capacity," FHWA/LA.17/640, [Online]. Available: https://rosap.ntl.bts.gov/view/dot/58439. [Accessed 22 August 2024].

[6]   R. Perez-Cartagena and A. Tarko, "Predicting Traffic Conditions at Indiana Signalized Intersections," *Jt. Transp. Res. Program*, p. 171, 2004.

[7]   "Traffic Signal Timing Manual: Chapter 3—Office of Operations," [Online]. Available: https://ops.fhwa.dot.gov/publications/fhwahop08024/chapter3.htm. [Accessed 14 January 2025].

[8]   J. Joseph and G. L. Chang, "Saturation Flow Rates and Maximum Critical Lane Volumes for Planning Applications in Maryland," *J. Transp. Eng.*, vol. 131, no. 12, December 2005, pp. 946–952, doi: 10.1061/(ASCE)0733-947X(2005)131:12(946).

[9] J. Bonneson, B. Nevers, J. Zegeer, T. Nguyen and T. Fong, "Guidelines for Quantifying the Influence of Area Type and Other Factors on Saturation Flow Rate," Texas Transportation Institute, College Station. TX, 2005, [Online]. Available: https://www.researchgate.net/profile/Jake-Zegeer/publication/237489163_Guidelines_for_Quantifying_the_Influence_of_Area_Type_and_Other_Factors_on_Saturation_Flow_Rate/links/5a03e20baca272b06ca64a4e/Guidelines-for-Quantifying-the-Influence-of-Area-Type-and-Other-Factors-on-Saturation-Flow-Rate.pdf. [Accessed 11 September 2024].

[10] B. M. Dunlap, "Field Measurement of Ideal Saturation Flow Rate from the Highway Capacity Manual," West Virginia University, 2005, [Online]. Available: https://search.proquest.com/openview/5216a7c6b6ccdb79156401fdf028dddd/1?pq-origsite=gscholar&cbl=18750&diss=y&casa_token=qg92pvAjbgIAAAAA:MITiyAmyztNCO-n-1lX5eN3aPZLRr29j8TWYgPpAWaHKxRUPyyVj_l1-aZZQOfgGj3s32hbN. [Accessed 11 September 2024].

[11] National Academies of Sciences and Medicine, *Highway Capacity Manual 7th Edition: A Guide for Multimodal Mobility Analysis*, 2022, [Online]. Available: https://nap.nationalacademies.org/catalog/26432/highway-capacity-manual-7th-edition-a-guide-for-multimodal-mobility. [Accessed 11 September 2024].

[12] K. Fitzpatrick, "Gaps Accepted at Stop-Controlled Intersections," *Transp. Res. Rec.*, vol. 1303, no. 11, pp. 103–112, 1991.

[13] "The Transportation Planning Process Briefing Book," United States Department of Transportation, Transportation Planning Capacity Building Program, FHWA-HEP-18-005, December 2019.

[14] F. V. Webster and J. Eaton, "A Method of Measuring Saturation Flow at Traffic Signals," Road Research Laboratory Road Note 34, Crowthorne, 1963.

[15] D. Branston and P. Gipps, "Some Experience with a Multiple Linear Regression Method of Estimating Parameters of the Traffic Signal Departure Process," *Transp. Res. Part Gen.*, vol. 15, no. 6, pp. 445–458, 1981.

[16] R. M. Kimber, M. McDonald and N. Hounsell, "Passenger Car Units in Saturation Flows: Concept, Definition, Derivation," *Transp. Res. Part B Methodol.*, vol. 19, no. 1, pp. 39–61, 1985.

[17] R. W. Stokes, V. G. Stover and C. J. Messer, "Use and Effectiveness of Simple Linear Regression to Estimate Saturation Flows at Signalized Intersections," *Transp. Res. Rec.*, vol. 1091, pp. 95–101, 1986.

[18] S. Mondal, V. K. Arya and A. Gupta, "An Optimised Approach for Saturation Flow Estimation of Signalised Intersections," *Proc. Inst. Civ. Eng. - Transp.*, vol. 175, no. 3, pp. 137–149, June 2022, doi: 10.1680/jtran.18.00206.

[19] C. C. Minh and K. Sano, "Analysis of Motorcycle Effects to Saturation Flow Rate at Signalized Intersection in Developing Countries," *J. East. Asia Soc. Transp. Stud.*, vol. 5, no. 10, pp. 1211–1222, 2003.

[20] X. Le, J. Lu, E. A. Mierzejewski and Y. Zhou, "Variations in Capacity at Signalized Intersections with Different Area Types," *Transp. Res. Rec. J. Transp. Res. Board*, vol. 1710, no. 1, pp. 199–204, January 2000, doi: 10.3141/1710-23.

[21] D. P. Allen, J. E. Hummer, N. M. Rouphail and J. S. Milazzo, "Effect of Bicycles on Capacity of Signalized Intersections," *Transp. Res. Rec.*, vol. 1646, no. 1, pp. 87–95, January 1998, doi: 10.3141/1646-11.

[22] J. S. Milazzo, N. M. Rouphail, J. E. Hummer and D. P. Allen, "Effect of Pedestrians on Capacity of Signalized Intersections," *Transp. Res. Rec.*, vol. 1646, no. 1, pp. 37–46, January 1998, doi: 10.3141/1646-05.

[23] D. Branston and H. van Zuylen, "The Estimation of Saturation Flow, Effective Green Time and Passenger Car Equivalents at Traffic Signals by Multiple Linear Regression," *Transp. Res.*, vol. 12, no. 1, pp. 47–53, February 1978, doi: 10.1016/0041-1647(78)90107-7.

[24] R. I. Perez-Cartagena and A. P. Tarko, "Calibration of Capacity Parameters for Signalized Intersections in Indiana," *J. Transp. Eng.*, vol. 131, no. 12, pp. 904–911, December 2005, doi: 10.1061/(ASCE)0733-947X(2005)131:12(904).

[25] H. Qi and X. Hu, "Real-time Headway State Identification and Saturation Flow Rate Estimation: A Hidden Markov Chain Model," *Transp. Transp. Sci.*, vol. 16, no. 3, pp. 840–864, January 2020, doi: 10.1080/23249935.2020.1722285.

[26] L. Wang, Y. Wang and Y. Bie, "Automatic Estimation Method for Intersection Saturation Flow Rate Based on Video Detector Data," *J. Adv. Transp.*, vol. 2018, pp. 1–9, July 2018, doi: 10.1155/2018/8353084.

[27] Y. Wang, J. Rong, C. Zhou and Y. Gao, "Dynamic Estimation of Saturation Flow Rate at Information-Rich Signalized Intersections," *Information*, vol. 11, no. 4, p. 178, 2020.

[28] J. W. McMahon, J. P. Krane and A. P. Federico, "Saturation Flow Rates by Facility Type," *Inst. Transp. Eng. ITE J.*, vol. 67, no. 1, p. 46, 1997.

[29] C. J. Bester and W. L. Meyers, "Saturation Flow Rates," *SATC 2007*, [Online]. Available: https://repository.up.ac.za/handle/2263/5838. [Accessed 12 September 2024].

[30] I. B. Potts, J. F. Ringert, K. M. Bauer, J. D. Zegeer, D. W. Harwood and D. K. Gilmore, "Relationship of Lane Width to Saturation Flow Rate on Urban and Suburban Signalized Intersection Approaches," *Transp. Res. Rec. J. Transp. Res. Board*, vol. 2027, no. 1, pp. 45–51, January 2007, doi: 10.3141/2027-06.

[31] C. Shao, J. Rong and X. Liu, "Study on the Saturation Flow Rate and Its Influence Factors at Signalized Intersections in China," *Procedia-Soc. Behav. Sci.*, vol. 16, pp. 504–514, 2011.

[32] B. W. Al-Mistarehi, A. H. Alomari and M. S. Al Zoubi, "Investigation of Saturation Flow Rate Using Video Camera at Signalized Intersections in Jordan," *Open Eng.*, vol. 11, no. 1, pp. 216–226, December 2020, doi: 10.1515/eng-2021-0021.

[33] J. D. Zegeer, "Field Validation of Intersection Capacity Factors," *Transp. Res. Rec.*, vol. 1091, pp. 67–77, 1986.

[34] M. M. Bruwer, C. J. Bester and E. S. Viljoen, "The Influence of Gradient on Saturation Flow Rate at Signalised Intersections," *J. South Afr. Inst. Civ. Eng.*, vol. 61, no. 2, pp. 21–27, 2019.

[35] M. Roshani and I. Bargegol, "Effect of Pedestrians on the Saturation Flow Rate of Right Turn Movements at Signalized Intersection—Case Study from Rasht City," in *IOP Conference Series: Materials Science and Engineering*, IOP Publishing, 2017, p. 042032. [Online]. Available: https://iopscience.iop.org/article/10.1088/1757-899X/245/4/042032/meta. [Accessed 12 September 2024].

[36] Y. Zhou, J. J. Lu, E. A. Mierzejewski and X. Le, "Development of Driver Population Factors for Capacity Analysis of Signalized Intersections," *Transp. Res. Rec. J. Transp. Res. Board*, vol. 1710, no. 1, pp. 239–245, January 2000, doi: 10.3141/1710-28.

[37] H. Sun, J. Yang, L. Wang, L. Li and B. Wu, "Saturation Flow Rate and Start-Up Lost Time of Dual-Left Lanes at Signalized Intersection in Rainy Weather Condition," *Procedia-Soc. Behav. Sci.*, vol. 96, pp. 270–279, 2013.

[38] B. H. Al-Omari and Y. B. Musa, "Estimation of Base Saturation Flow Rates for Signalized Intersections in Jordan and Kuwait," *J. Eng. Appl. Sci.*, vol. 15, no. 24, 2020, [Online]. Available: https://www.researchgate.net/profile/Bashar-Al-Omari/publication/349297516_ESTIMATION_OF_BASE_SATURATION_FLOW_RATES_FOR_SIGNALIZED_INTERSECTIONS_IN_JORDAN_AND_KUWAIT/links/6028eb4ea6fdcc37a824f94b/ESTIMATION-OF-BASE-SATURATION-FLOW-RATES-FOR-SIGNALIZED-INTERSECTIONS-IN-JORDAN-AND-KUWAIT.pdf. [Accessed 12 September 2024].

[39] J. A. Bonneson and C. J. Messer, "Phase Capacity Characteristics for Signalized Interchange and Intersection Approaches," *Transp. Res. Rec. J. Transp. Res. Board*, vol. 1646, no. 1, pp. 96–105, January 1998, doi: 10.3141/1646-12.

[40] J. A. Bonneson, "Study of Headway and Lost Time at Single-Point Urban Interchanges," *Highway Capacity*, vol. 32, 1993, [Online]. Available: https://onlinepubs.trb.org/Onlinepubs/trr/1992/1365/1365.pdf#page=36. [Accessed 10 September 2024].

[41] K. R. Agent and J. D. Crabtree, "Analysis of Saturation Flow at Signalized Intersections," 1982, [Online]. Available: https://uknowledge.uky.edu/ktc_researchreports/761/. [Accessed 11 September 2024].

[42] C. Lee and M. Abdel-Aty, "Presence of Passengers: Does It Increase or Reduce Driver's Crash Potential?" *Accid. Anal. Prev.*, vol. 40, no. 5, pp. 1703–1712, September 2008, doi: 10.1016/j.aap.2008.06.006.

[43] A. P. Tarko and M. Tracz, "Uncertainty in Saturation Flow Predictions," *Red*, vol. 1, no. 2, 2000, [Online]. Available: https://onlinepubs.trb.org/Onlinepubs/circulars/EC018/27_46.pdf. [Accessed 11 September 2024].

[44] R. G. Dowling, "Use of Default Parameters for Estimating Signalized Intersection Level of Service," *Transp. Res. Rec.*, vol. 1457, pp. 82–95, 1994.

[45] Z. Khatib and M. Kyte, "Framework to Consider the Effect of Uncertainty in Forecasting the Level of Service of Signalized and Unsignalized Intersections," in *Transportation Research Circular*, June 2000. [Online]. Available: https://trid.trb.org/View/657356. [Accessed 11 September 2024].

[46] K. Hamad and H. Abuhamda, "Estimating Base Saturation Flow Rate for Selected Signalized Intersections in Doha, Qatar," *J. Traffic Logist. Eng.*, vol. 3, no. 2, 2015, [Online]. Available: http://www.jtle.net/uploadfile/2015/0826/20150826021325831.pdf. [Accessed 12 September 2024].

[47] M. J. B. Alam, K. A. Osra, H. O. Al-Bar and S. Z. Zahran, "Signalized Intersection Capacity Adjustment Factors for Makkah, Saudi Arabia," *Can. J. Transp.*, vol. 4, no. 1, Art. no. 1, 2010, [Online]. Available: https://journalhosting.ucalgary.ca/index.php/cjt/article/view/15839. [Accessed 11 September 2024].

[48] M. M. Rahman, S. N. Ahmed and T. Hassan, "Comparison of Saturation Flow Rate at Signalized Intersections in Yokohama and Dhaka," in *Proceedings of the Eastern Asia Society for Transportation Studies*, 2005, pp. 959–966. [Online]. Available: https://www.academia.edu/download/78216985/COMPARISON_OF_SATURATION_FLOW_RATE_AT_SI20220106-11097-14jdp7k.pdf. [Accessed 12 September 2024].

[49] R. J. Troutbeck, "Estimating the Critical Acceptance Gap from Traffic Movements: Research Report No 92-5," *Qld. Univ. Technol. Brisb. Qld. Aust.*, 1992.

[50] M. S. Raff, "A Volume Warrant for Urban Stop Signs," 1950, [Online]. Available: https://rosap.ntl.bts.gov/view/dot/16265. [Accessed 13 September 2024].

[51] X. J. Dai, "The Impact of Driving Behavior of Older Drivers on Intersection Capacity," *Res. Rep. Dep. Civ. Environ. Eng.*, 1997, [Online]. Available: https://cir.nii.ac.jp/crid/1570572699500360320. [Accessed 13 September 2024].

[52] S. Dissanayake, J. J. Lu and Y. I. Ping, "Driver Age Differences in Day and Night Gap Acceptance Capabilities," *Iatss Res.*, vol. 26, no. 1, pp. 71–79, 2002.

[53] W. K. Kittelson and M. A. Vandehey, "Delay Effects on Driver Gap Acceptance Characteristics at Two-Way Stop-Controlled Intersections," *Transp. Res. Rec.*, no. 1320, 1991, [Online]. Available: https://trid.trb.org/View/365598. [Accessed 13 September 2024].

[54] S. Mullapudi and J. J. Lu, "Capacity Reduction Due to Older Drivers at Stop-Controlled Intersections: A Research Report," 1998, [Online]. Available: https://trid.trb.org/View/579252. [Accessed 13 September 2024].

[55] P. Yi, "Gap Acceptance for Elderly Drivers on Rural Highways," in *Compendium of Technical Papers for the 66th ITE Annual Meeting Institute of Transportation Engineers (ITE)*, 1996, [Online]. Available: https://trid.trb.org/View/481613. [Accessed 13 September 2024].

[56] Z. Tian et al., "Implementing the Maximum Likelihood Methodology to Measure a Driver's Critical Gap," *Transp. Res. Part Policy Pract.*, vol. 33, no. 3–4, pp. 187–197, 1999.

[57] M. Kyte, W. Kittelson, Z. Tian, W. Brilon, R. Troutbeck and S. Mir, "New Measurements for Saturation Headways and Critical Gaps at Stop-Controlled Intersections," in *Proc., 2nd Int. Symp. on Highway Capacity at Sydney*, Austrialian Road Research Board, Melbourne, Australia, 1994, pp. 345–364, [Online]. Available: https://www.academia.edu/download/113501733/kyte-new_measurements_for_saturation_headways.pdf. [Accessed 13 September 2024].

[58] B. D. Greenshields, D. Schapiro and E. L. Ericksen, "Traffic Performance at Urban Street Intersections," 1946, [Online]. Available: https://trid.trb.org/View/117305. [Accessed 13 September 2024].

[59] J. L. Gattis and S. T. Low, "Gap Acceptance at Atypical Stop-Controlled Intersections," *J. Transp. Eng.*, vol. 125, no. 3, pp. 201–207, May 1999, doi: 10.1061/(ASCE)0733-947X(1999)125:3(201).

[60] D. W. Harwood, J. M. Mason Jr., and K. Fitzpatrick, "Field Observations of Truck Operational Characteristics Related to Intersection Sight Distance," *Transp. Res. Rec.*, no. 1280, 1990, [Online]. Available: https://trid.trb.org/View/352819. [Accessed 13 September 2024].

[61] A. J. Miller, "Nine Estimators of Gap-Acceptance Parameters," *Publ. Traffic Flow Transp.*, 1971, [Online]. Available: https://trid.trb.org/View/122875. [Accessed 13 September 2024].

[62] S. M. Madanat, M. J. Cassidy and M. Wang, "Probabilistic Delay Model at Stop-Controlled Intersection," *J. Transp. Eng.*, vol. 120, no. 1, pp. 21–36, January 1994, doi: 10.1061/(ASCE)0733-947X(1994)120:1(21).

[63] W. Brilon, R. Koenig and R. J. Troutbeck, "Useful Estimation Procedures for Critical Gaps," *Transp. Res. Part Policy Pract.*, vol. 33, no. 3–4, pp. 161–186, 1999.

[64] A. Weinert, "Estimation of Critical Gaps and Follow-Up Times at Rural Unsignalized Intersections in Germany," in *Fourth International Symposium on Highway Capacity*, 2000, pp. 409–421, [Online]. Available: https://onlinepubs.trb.org/Onlinepubs/circulars/ec018/35_37.pdf. [Accessed 13 September 2024].

[65] L. M. Blogg et al., "NCHRP Report 572: Roundabouts in the United States," *Transp. Res. Board*, 2007.

[66] N. Wu, "A New Model for Estimating Critical Gap and Its Distribution at Unsignalized Intersections Based on the Equilibrium of Probabilities," in *Proceeding of the 5th International Symposium on Highway Capacity and Quality of Service. Yokohama, Japan*, 2006, [Online]. Available: https://www.researchgate.net/profile/Ning-Wu/publication/238664405_A_NEW_MODEL_FOR_ESTIMATING_CRITICAL_GAP_AND_ITS_DISTRIBUTION_AT_UNSIGNALIZED_INTERSECTIONS_BASED_ON_THE_EQUILIBRIUM_OF_PROBABILITIES/links/0deec52a1ac898ff63000000/A-NEW-MODEL-FOR-ESTIMATING-CRITICAL-GAP-AND-ITS-DISTRIBUTION-AT-UNSIGNALIZED-INTERSECTIONS-BASED-ON-THE-EQUILIBRIUM-OF-PROBABILITIES.pdf. [Accessed 13 September 2024].

[67] R. J. Troutbeck, "Estimating the Mean Critical Gap," *Transp. Res. Rec. J. Transp. Res. Board*, vol. 2461, no. 1, pp. 76–84, January 2014, doi: 10.3141/2461-10.

[68] R. J. Troutbeck, "Revised Raff's Method for Estimating Critical Gaps," *Transp. Res. Rec. J. Transp. Res. Board*, vol. 2553, no. 1, pp. 1–9, January 2016, doi: 10.3141/2553-01.

[69] P. McGowen and L. Stanley, "Alternative Methodology for Determining Gap Acceptance for Two-Way Stop-Controlled Intersections," *J. Transp. Eng.*, vol. 138, no. 5, pp. 495–501, May 2012, doi: 10.1061/(ASCE)TE.1943-5436.0000358.

[70] D. S. Pawar and G. R. Patil, "Analyzing Variations in Spatial Critical Gaps at Two-Way Stop-Controlled Intersections Using Parametric and Non-Parametric Techniques," *J. Traffic Transp. Eng. Engl. Ed.*, vol. 8, no. 1, pp. 129–138, 2021.

[71] M. Mohan and S. Chandra, "Critical Gap Estimation at Two-Way Stop-Controlled Intersections Based on Occupancy Time Data," *Transp. Transp. Sci.*, vol. 14, no. 4, pp. 316–329, April 2018, doi: 10.1080/23249935.2017.1385657.

[72] M. Kyte, C. Clemow, N. Mahfood, B. K. Lall and C. J. Khisty, "Capacity and Delay Characteristics of Two-Way Stop-Controlled Intersections," *Transp. Res. Rec.*, vol. 1320, pp. 160–167, 1991.

[73] S. M. Tupper, M. A. Knodler Jr. and D. S. Hurwitz, "Connecting Gap Acceptance Behavior with Crash Experience," in *3rd International Conference on Road Safety and Simulation, Purdue University, Transportation Research Board*, 2011, [Online]. Available: https://trid.trb.org/View/1285691. [Accessed 13 September 2024].

[74] Z. Z. Tian et al., "A Further Investigation on Critical Gap and Follow-Up Time," in *Proceedings of the 4th International Symposium on Highway Capacity, Maui/Hawaii, Transportation Research Circular E-C018*, 2000, pp. 409–421, [Online]. Available: https://onlinepubs.trb.org/Onlinepubs/circulars/EC018/34_45.pdf. [Accessed 13 September 2024].

[75] W. Brilon, R. Koenig and R. J. Troutbeck, "Useful Estimation Procedures for Critical Gaps," *Transp. Res. Part Policy Pract.*, vol. 33, no. 3–4, pp. 161–186, 1999.

[76] R. J. Troutbeck, "Estimating the Mean Critical Gap," *Transp. Res. Rec. J. Transp. Res. Board*, vol. 2461, no. 1, pp. 76–84, January 2014, doi: 10.3141/2461-10.

[77] R. J. Troutbeck, "Revised Raff's Method for Estimating Critical Gaps," *Transp. Res. Rec. J. Transp. Res. Board*, vol. 2553, no. 1, pp. 1–9, January 2016, doi: 10.3141/2553-01.

[78] D. Kiptoon, "Feature Selection in Machine Learning," Medium, [Online]. Available: https://medium.com/@jdkiptoon/feature-selection-in-machine-learning-20417d052b80. [Accessed 17 January 2025].

[79] M. Kuhn, "Applied Predictive Modeling," Springer, 2013, [Online]. Available: https://mathematics.foi.hr/Rprojekti/knjige/applied-predictive-modeling-max-kuhn-kjell-johnson.pdf. [Accessed 17 January 2025].

[80] "Capacity and Saturation Flow Rate," [Online]. Available: https://www.webpages.uidaho.edu/niatt_labmanual/Chapters/signaltimingdesign/theory andconcepts/CapacityAndSaturationFlowRate.htm. [Accessed 25 March 2025].

[81] M. Patkar, "Effect of On-Street Width and Capacity of Urba," [Online]. Available: https://www.istiee.unict.it/europeantransport/papers/N73/P01_73_2019.pdf. [Accessed 25 March 2025].

[82] "Full Article: Lane-Based Analysis of the Saturation Flow Rate Considering Traffic Composition," [Online]. Available: https://www.tandfonline.com/doi/full/10.1080/03081060.2023.2214144#abstract. [Accessed 17 January 2025].

[83] "Western Uniformity Scenario Analysis—Chapter VIII Traffic Operations," [Online]. Available: https://www.fhwa.dot.gov/policy/otps/truck/wusr/chap08.cfm. [Accessed 17 January 2025].

[84] D. Kong, X. Guo, B. Yang and D. Wu, "Analyzing the Impact of Trucks on Traffic Flow Based on an Improved Cellular Automaton Model," *Discrete Dyn. Nat. Soc.*, vol. 2016, no. 1, p. 1236846, 2016, doi: 10.1155/2016/1236846.

[85] "Types of Problems at Unsignalized Intersections—Unsignalized Intersection Improvement Guide," [Online]. Available: https://toolkits.ite.org/uiig/problems.aspx. [Accessed 7 March 2025].

[86] "Average Speeds Increase After Utah Raises Limit to 80 mph," IIHS-HLDI Crash Testing and Highway Safety, [Online]. Available: https://www.iihs.org/news/detail/average-speeds-increase-after-utah-raises-limit-to-80-mph. [Accessed 7 March 2025].

[87] "Index—Synthesis of Safety Research Related to Speed and Speed Management, July 1998—FHWA-RD-98-154," [Online]. Available: https://www.fhwa.dot.gov/publications/research/safety/98154/speed.cfm. [Accessed 7 March 2025].

Appendix

Appendix A: countCAM4 Details

countCAM4 Capability

Designed and assembled in the U.S. by StreetLogic Pro, the countCAM4 is a compact, lightweight traffic counting camera weighing only 2.8 lbs. It is easily deployable and allows users to collect multiple days of video data on a single device. Additionally, it can collect directional vehicular volume. The countCAM4 features dual modes of data collection: counter mode for direction, speed, and volume, and camera mode for video data collection [80].

The countCAM4 does not require users to interact with traffic while collecting data, providing the survey team with greater flexibility and ensuring their safety. Its setup time is very short, taking less than 3 min. The smart technology used in this device optimizes computing power, enabling the camera to run for up to 100 continuous hrs. without external batteries, allowing for the collection of traffic data over multiple consecutive days. This equipment is also highly durable, having been tested for industrial-grade resilience to withstand heat, snow, rain, and drops. It operates reliably in both rainy and snowy weather conditions [80].

Figure 31. countCAM4

The countCAM4 utilizes GPS to set the date and time, requiring an initial GPS lock to ensure accurate synchronization with the user's time zone, a process necessary only during the first use or when switching time zones. It communicates with WiFi-enabled devices via a local wireless network and allows users to choose specific hours for recording. The countCAM4 offers five recording quality options, including 10fps Low Quality (480x360), 10fps Balanced (640x480), and 25fps Balanced (640x480), with the recommended setting being 10fps Balanced quality [81].

Installation of countCAM4

When in camera mode, the countCAM4 should be installed on a signpost or utility pole. It is recommended that the camera be positioned 50-150 ft. away from the center of the intersection to ensure all movements are visible within the camera's view. There should be no objects in front of the camera that might obstruct the view [81].

When in Counter Mode, the countCAM4 should be installed on a signpost or utility pole next to the two-lane roadway where data is to be collected. The countCAM4 camera lens should be positioned 3 to 5 ft. above the roadway surface and oriented perpendicular to the roadway. To ensure accurate traffic volume counts, the device should be placed at least 6 ft. away from the closest vehicle. For accurate speed data collection, this distance should be increased to approximately 15 ft. from the nearest lane for traffic moving at 35 mph or less, and

approximately 20 ft. for traffic moving at 40 mph or greater. Additionally, the countCAM4 should not be pointed at locations where busy sidewalks, driveways, or other roads are visible in the background, as the device detects all objects in its field of view and can overcount in these situations [81].

Figure A32. Installed countCAM4

countCLOUD

Provided by the same company, StreetLogic Pro, countCLOUD is a traffic video processing system that offers an accurate, quick, simple, and cost-effective way to analyze traffic videos into meaningful data. It provides precise point counts and turning movement counts with 95-98% accuracy, along with options for 2-, 3-, and 13-class vehicle turning movement counts, point counts, or pedestrian/bike trail count processing. After uploading the video data on the system, a comprehensive report is prepared within three business days. The system features an interactive and user-friendly central dashboard that allows users to navigate and manage traffic counts efficiently. Users can add and configure counts of any length to match their needs. Additionally, it includes features such as project overviews and user additions. Overall, this system offers a convenient and cost-saving method for processing traffic counts from video data, reducing both time and complexity [82].

Appendix B: Example Adjustment for BSFR

Figure A33. Example of adjustment of SFR